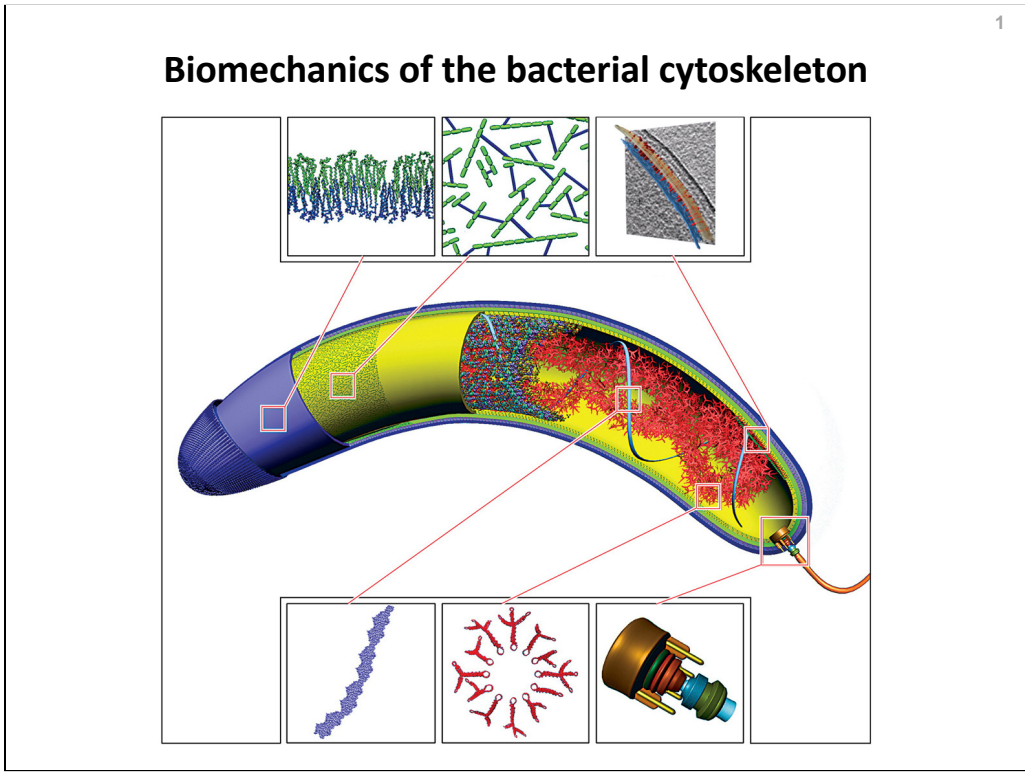

Source: Morris DM, Jensen GJ (2008) Towards a biomechanical understanding of whole bacterial cells. *Annu Rev Biochem* 77: 583-613 PMID: 18355161.

Figure 1. Overview of bacterial ultrastructure. The main image shows successive cutaway views of the S-layer, outer membrane, peptidoglycan, inner membrane, protein-rich cytoplasm, and supercoiled DNA. Clockwise from top left, the zoom boxes depict: lipid bilayer; peptidoglycan; chemoreceptor cluster; flagellar motor; supercoiled domains on the bacterial chromosome; MreB protofilament.

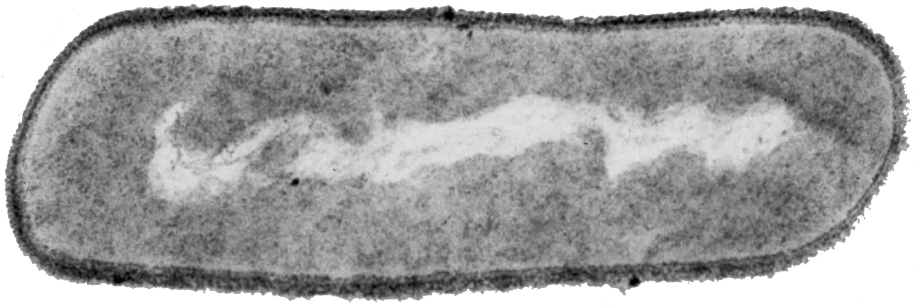

"This [bacterial] cell interior appears as a matrix of varying texture without any obvious organized interior structure."

Source: Alberts et al. (2002) *Molecular Biology of the Cell* (4th Edition).

We now know that the interior of a bacterial cell is anything but “disorganized” – on the contrary! The bacterial cytoskeleton is one of the main determinants of the internal order of bacterial cells. Until recently, however – as reflected in this statement from the 2002 edition of the classic textbook by Bruce Alberts and colleagues – it was thought that bacteria did not possess a cytoskeleton. Since then, microbiologists have discovered that not only do bacteria possess a cytoskeleton, the family of bacterial cytoskeleton proteins is actually larger and more diverse than the family of eukaryotic cytoskeleton proteins.

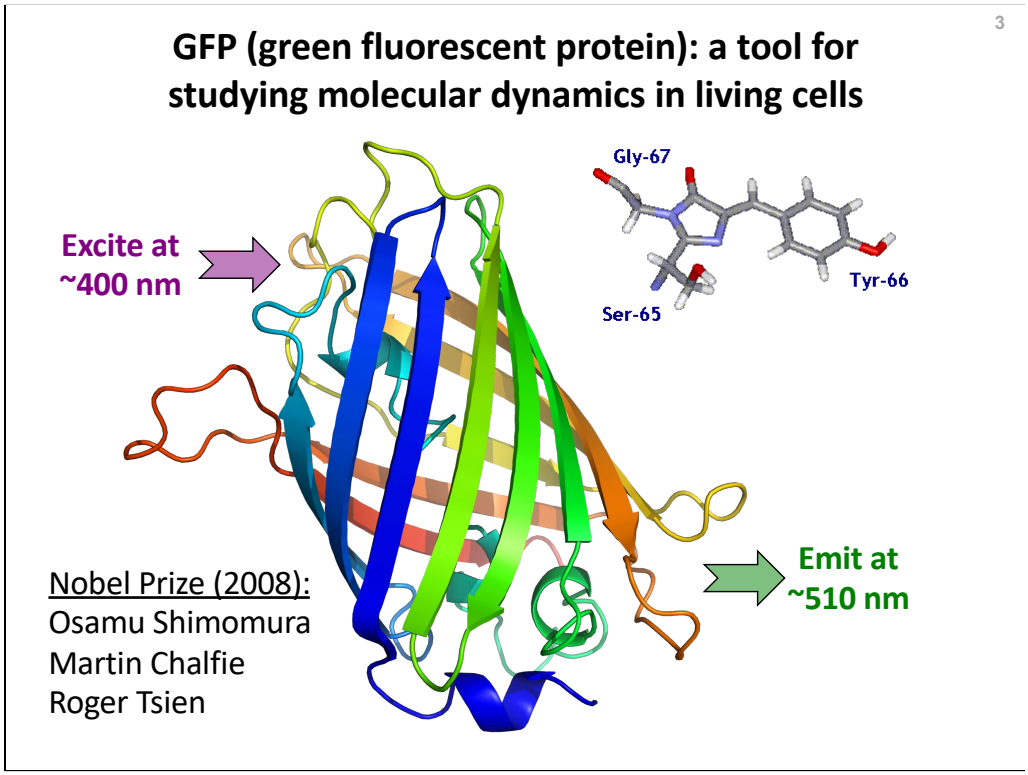

Source: http://core.biotech.hawaii.edu/gfp.htm.

One of the "key players" that has allowed microbiologists to study the assembly, localization, and dynamics of bacterial cytoskeletal proteins in living bacterial cells is the discovery and exploitation of GFP (green fluorescent protein) and related fluorescent proteins with different excitation/emission spectra. By fusing GFP (or some other fluorescent protein) to a bacterial protein and expressing it in a living cell (see slide 5), the experimenter can track the assembly, localization, and dynamics of bacterial cytoskeletal proteins in living bacterial cells.

Source: https://www.nobelprize.org/prizes/chemistry/2008/press-release/

The Royal Swedish Academy of Sciences awarded the 2008 Nobel Prize in Chemistry jointly to: **Osamu Shimomura**, Marine Biological Laboratory (MBL), Woods Hole, MA, USA and Boston University Medical School, MA, USA; **Martin Chalfie**, Columbia University, New York, NY, USA; **Roger Y. Tsien**, Howard Hughes Medical Institute, University of California, San Diego, La Jolla, CA, USA for the discovery and development of the green fluorescent protein (GFP).

Fluorescent proteins (FPs) exist in a wide spectrum of chromatic variants

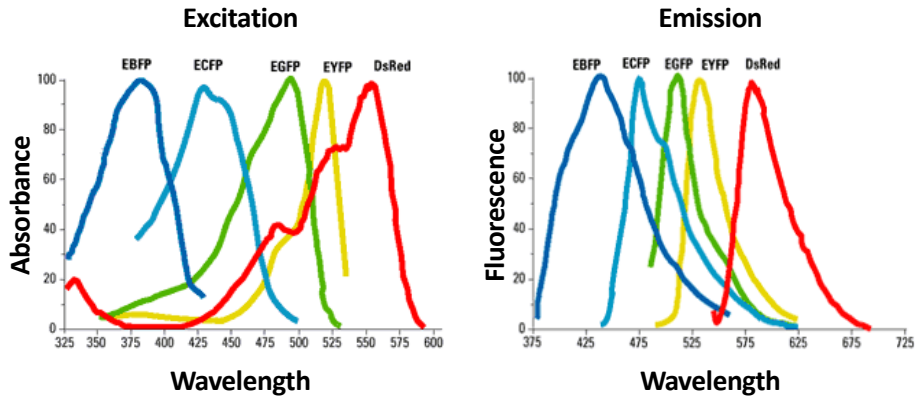

Source: https://deepgreen.dpb.carnegiescience.edu/cell%20imaging%20site%20/html/dual%20fp%20imaging.html

Excitation and emission spectra of some fluorescent proteins (FP): Blue (EBFP); Cyan (ECFP); Green (EGFP); Yellow (EYFP); Red (DsRed). And many others…

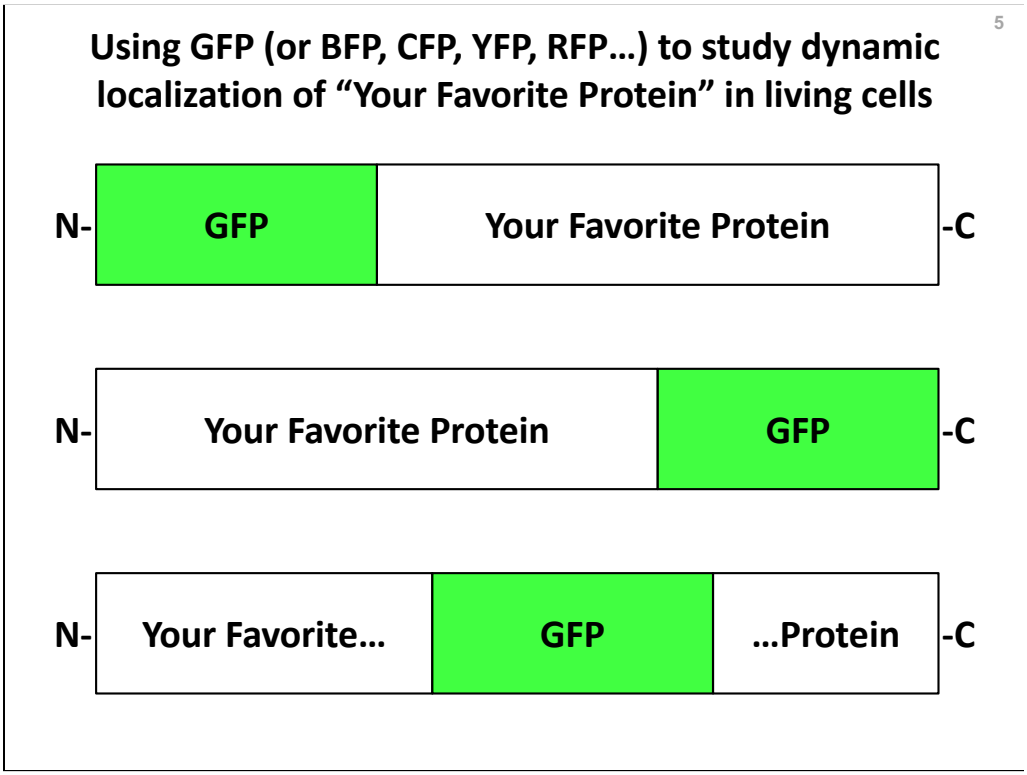

The open reading frame (ORF) encoding GFP or another chromatic variant of fluorescent protein (see slide 4) can be fused to the N-terminus (upper panel) or C-terminus (middle panel) of the ORF encoding Your Favorite Protein or even, in some cases, can be inserted into the ORF encoding Your Favorite Protein (lower panel).

The eukaryotic cytoskeleton: three major players

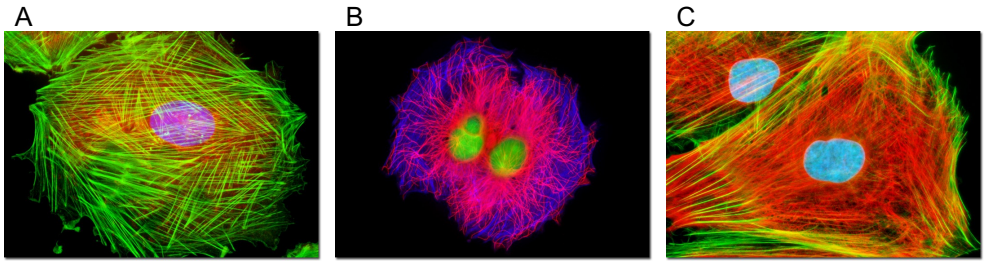

Actin microfilaments (green)	Tubulin microtubules (red)	Intermediate filaments (red)
Dynamic	**Dynamic**	**Static**

Source: http://micro.magnet.fsu.edu/primer/techniques/fluorescence/gallery/cells/a10/a10cells.html

(A-C) Embryonic Rat Thoracic Aorta Medial Layer Myoblast Cells (a.k.a. A-10 cells).

(A) Red: Unpolymerized globular (G) actin, which accumulates in the center of the cell, was stained with the fluorochrome Texas Red. **Green:** Polymerized filamentous (F) actin cytoskeletal network was labelled with Alexa Fluor 488 conjugated to phalloidin. **Blue:** DNA was stained with the ultraviolet-absorbing probe DAPI.

(B) Red: Microtubules were immunofluorescently labeled with mouse anti-α-tubulin primary antibodies followed by goat anti-mouse secondary antibodies conjugated to Alexa Fluor 568. Blue: Polymerized filamentous (F) actin was stained with phalloidin conjugated to Alexa Fluor 350. Green: DNA was stained with SYTOX Green.

(C) Red: Intermediate filaments were immunofluorescently labeled with mouse anti-vimentin primary antibodies followed by goat anti-mouse secondary antibodies conjugated to Texas Red-X. **Green:** Polymerized filamentous (F) actin was stained with phalloidin conjugated to Oregon Green 488. **Blue:** DNA was stained with Hoechst 33258.

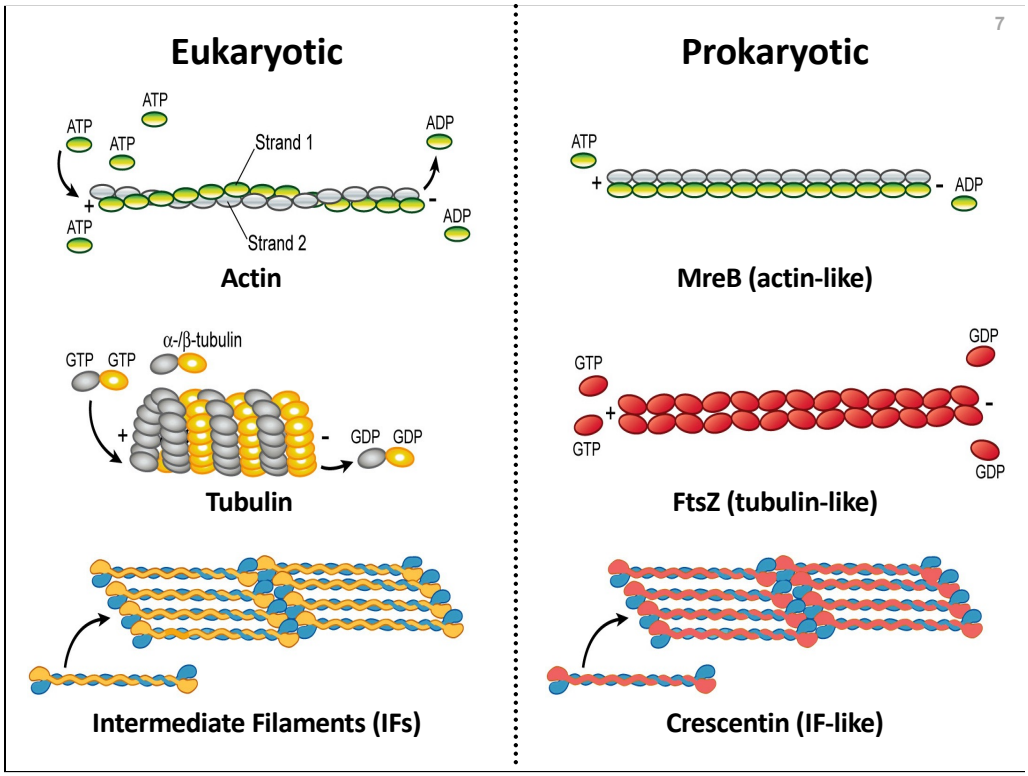

Source: Graumann PL (2007) Cytoskeletal elements in bacteria. *Annu Rev Microbiol* 61: 589-618 PMID: 17506674.

Figure 1. Schematic drawing of cytoskeletal elements:

Eukaryotic	Prokaryotic Homolog (Selected Example)
Actin	MreB
Tubulin	FtsZ
Intermediate Filaments	Crescentin

The eukaryotic cytoskeleton: actin microfilaments

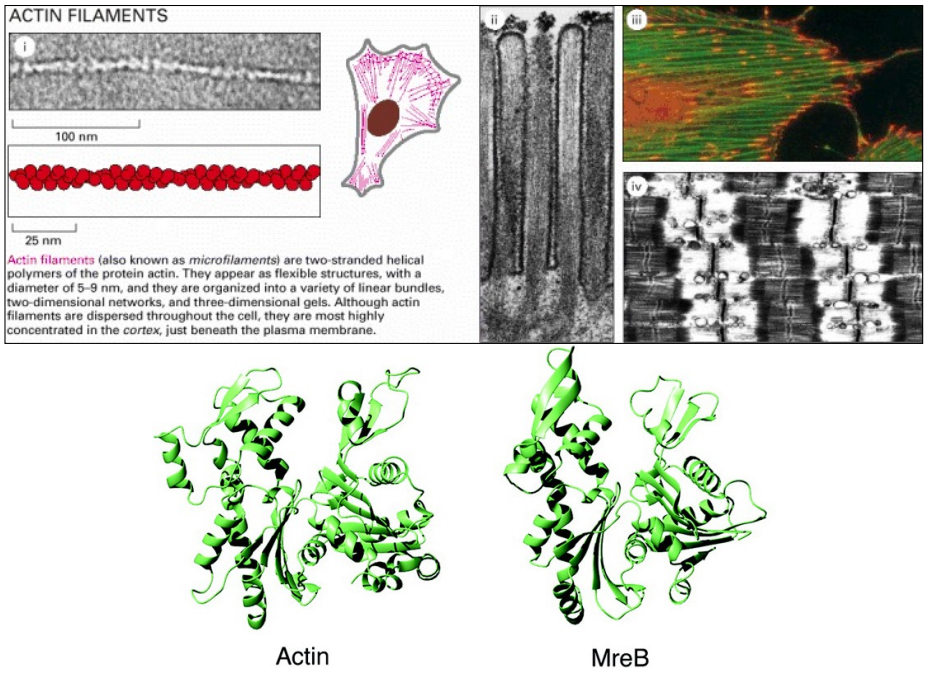

Source: http://www.ncbi.nlm.nih.gov/books/bv.fcgi?rid=mboc4.box.2958.

Figure 16-1. The three major types of protein that form the eukaryotic cytoskeleton: actin microfilaments (shown on this slide), tubulin microtubules, and intermediate filaments.

Source: Shih YL, Rothfield L (2006) The bacterial cytoskeleton. *Microbiol Mol Biol Rev.* 70(3): 729-754 PMID: 16959967.

Source: https://www.ncbi.nlm.nih.gov/books/NBK9841/

Figure 1. Structural comparison of eukaryotic actin and prokaryotic (bacterial) actin-like cytoskeletal proteins. Left: Eukaryotic actin from *Saccharomyces cerevisiae*. Right: Bacterial actin-like protein MreB from *Thermotoga maritima*. Note the clear structural similarity between the two proteins, despite the evolutionary divergence of eukaryotic and bacterial lineages at least 2.7 billion years ago, following some 1.0 to 1.5 billion years of prokaryotic evolution.

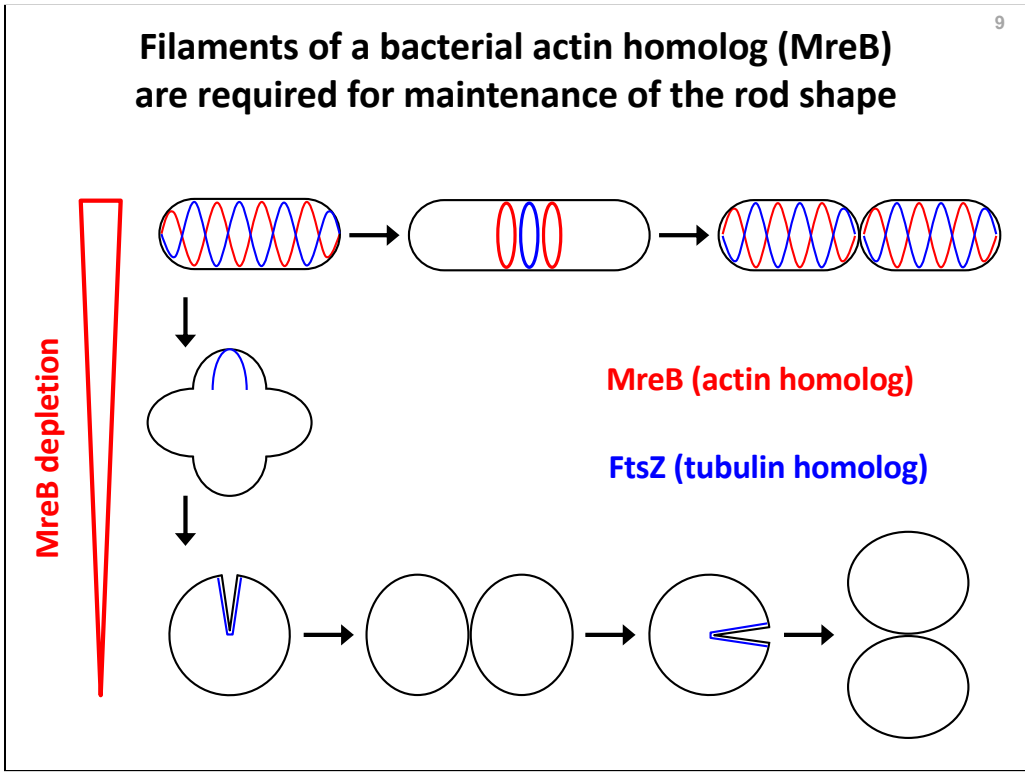

Source: Margolin M (2009) Sculpting the bacterial cell. *Curr Biol* 19(17): R812-R822 PMID: 19906583.

Figure 2. Roles for the actin-like MreB protein (red) and tubulin-like FtsZ protein (blue) in shaping bacterial cells.

Top row. During normal bacterial cell growth and division, FtsZ and MreB localize as hoops or helices wrapped around the short axis of the cell. When cells prepare to divide these helices collapse into a single FtsZ ring flanked by two MreB rings. After division, the FtsZ and MreB rings return to the original configuration.

Middle row. Depletion of MreB (indicated by the inverted red triangle) disrupts the MreB cytoskeleton and causes cells to become spheroidal over time.

Bottom row. MreB-depleted cells continue to grow, forming FtsZ arcs (blue) and then dividing at those arcs to form to form two spherical cells capable of growing and dividing again. MreB-depleted cells continue to grow and divide as spheroids, although they are not very "happy" (i.e., growth is extremely slow compared to normal rod-shaped cells and loss of chromosomal integrity occurs at very high frequencies).

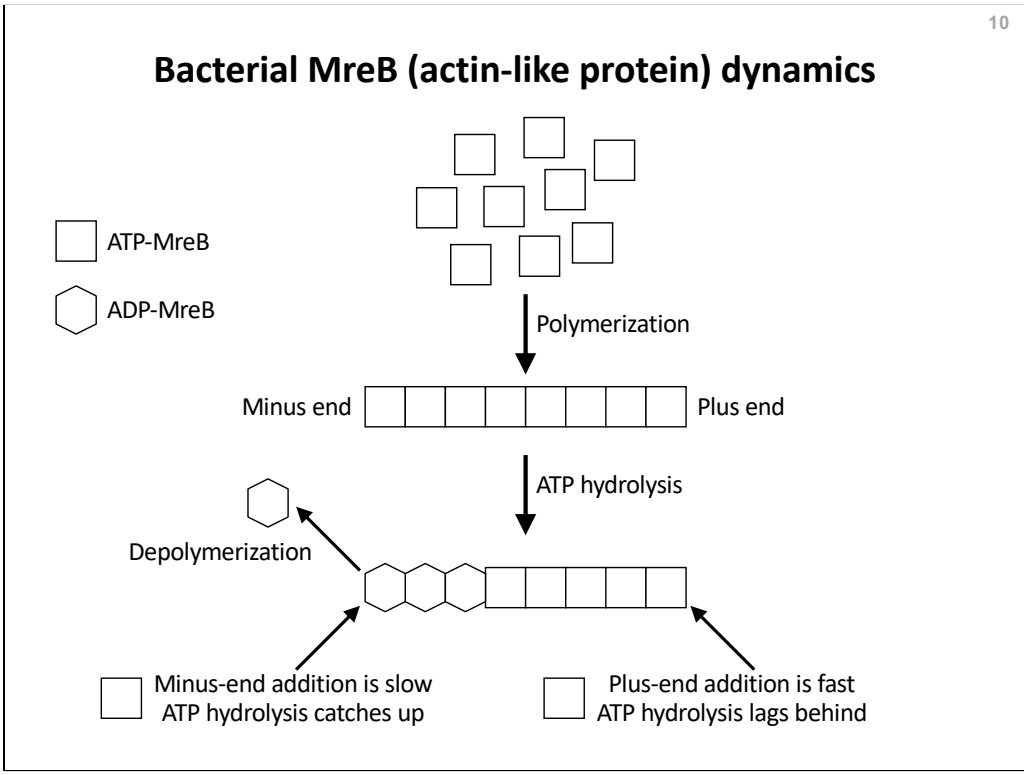

Source: http://www.ncbi.nlm.nih.gov/books/bv.fcgi?rid=mboc4.box.2958

Explanation for the different critical concentrations (C_c) at the plus and minus ends of a bacterial actin-like protein microfilament (e.g., MreB). MreB subunits can exist in ATP-bound form (squares) or ADP-bound form (hexagons). Subunits bound to ATP (ATP-MreB) polymerize at both ends of a growing filament, and then undergo nucleotide hydrolysis in the filament lattice. In this example, as the filament grows, elongation is faster than hydrolysis at the "plus end" and the terminal subunits at this end are therefore always in the ATP-MreB form. However, hydrolysis is faster than elongation at the "minus end", and so terminal subunits at this end are in the ADP-MreB form. Treadmilling occurs at intermediate concentrations of free subunits. The critical concentration for polymerization on a filament ending in the ATP-MreB form is lower than for a filament ending in the ADP-MreB form. If the actual subunit concentration is somewhere between these two values, the plus end grows while the minus end shrinks, resulting in treadmilling.

In the scientific literature, the "minus end" is also known as the "pointed end". The "plus end" is also known as the "barbed end". These names are based on electron microscopy images of actin filaments.

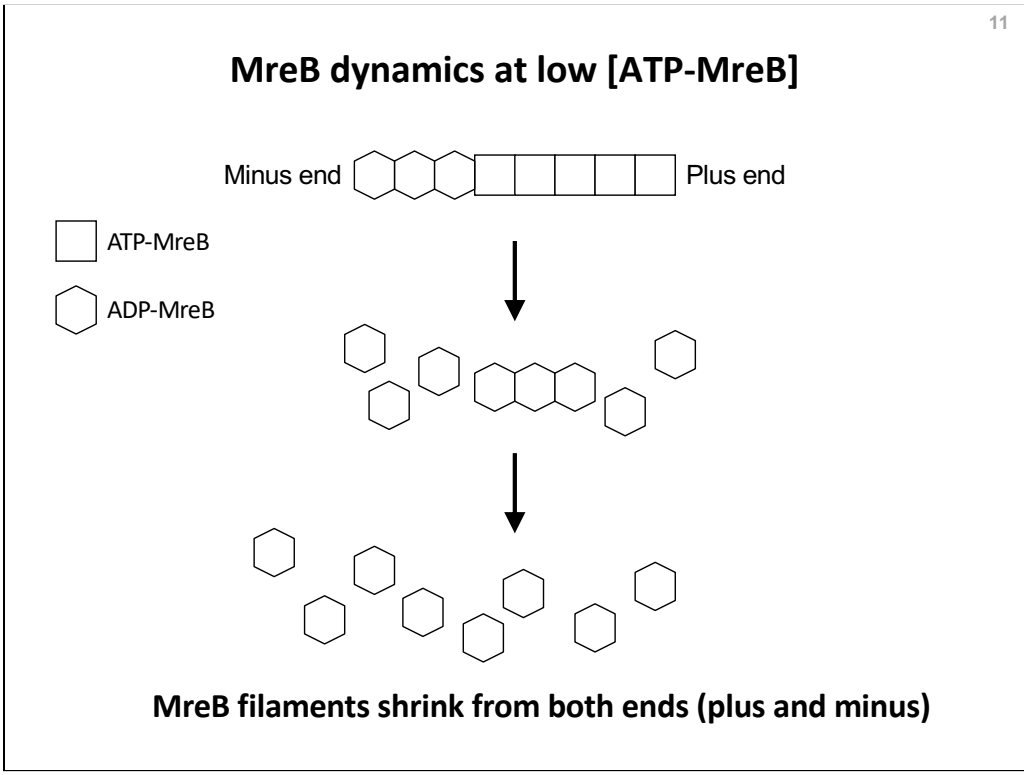

At **low concentrations** of free ATP-MreB, the rate of ATP hydrolysis at both ends (plus and minus) of the MreB filament is faster than the rate of addition of ATP-MreB subunits at both ends (plus and minus) of the MreB filament. Consequently, both ends of the MreB filament are "capped" with ADP-MreB subunits and there is a net subtraction of ADP-MreB subunits from both ends (plus and minus) of the MreB filament.

In sum: at **low concentrations** of free ATP-MreB, the MreB filament shrinks from both ends (plus and minus).

MreB dynamics at high [ATP-MreB]

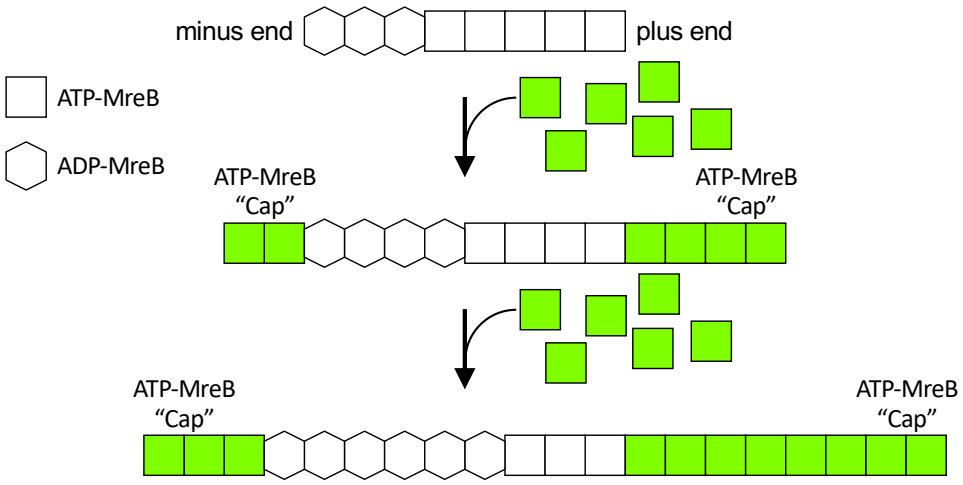

MreB filaments grow from both ends (plus and minus)

At **high concentrations** of free ATP-MreB, the rate of addition of ATP-MreB subunits at both ends (plus and minus) of the MreB filament is faster than the rate of ATP hydrolysis at both ends (plus and minus) of the MreB filament. Consequently, both ends of the MreB filament are "capped" with ATP-MreB subunits and there is a net addition of ATP-MreB subunits at both ends (plus and minus) of the MreB filament.

In sum: at **high concentrations** of free ATP-MreB, the MreB filament grows from both ends (plus and minus).

MreB "treadmilling" at intermediate [ATP-MreB]

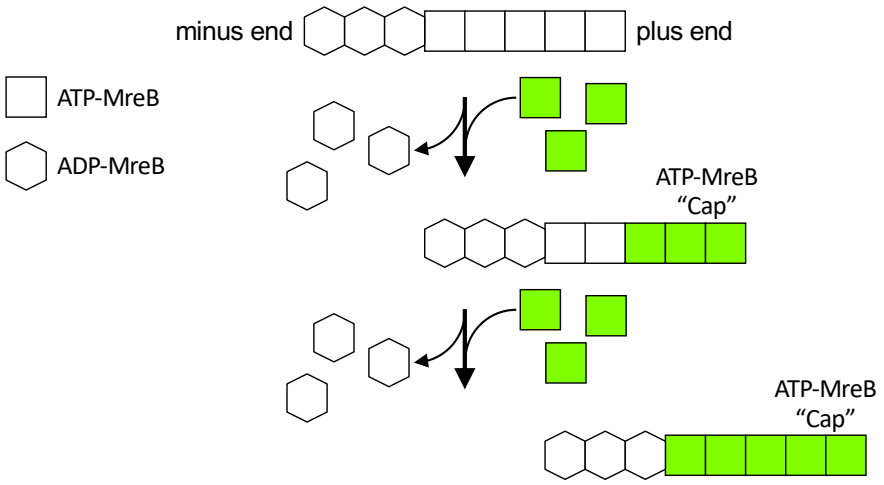

MreB filaments grow from plus end and shrink from minus end

At **intermediate concentrations** of free ATP-MreB, the plus and minus ends of the MreB filament behave differently!

Plus end. The rate of addition of ATP-MreB subunits at the **plus end** of the MreB filament is faster than the rate of ATP hydrolysis at the plus end. Consequently, the plus end of the MreB filament is "capped" with ATP-MreB subunits and there is a net addition of ATP-MreB subunits at the plus end of the MreB filament.

Minus end. The rate of addition of ATP-MreB subunits at the **minus end** of the MreB filament is slower than the rate of ATP hydrolysis at the minus end. Consequently, the minus end of the MreB filament is "capped" with ADP-MreB subunits and there is a net subtraction of ADP-MreB subunits at the minus end of the MreB filament.

In sum: at **intermediate concentrations** of free ATP-MreB, the MreB filament grows from the plus end and shrinks from the minus end.

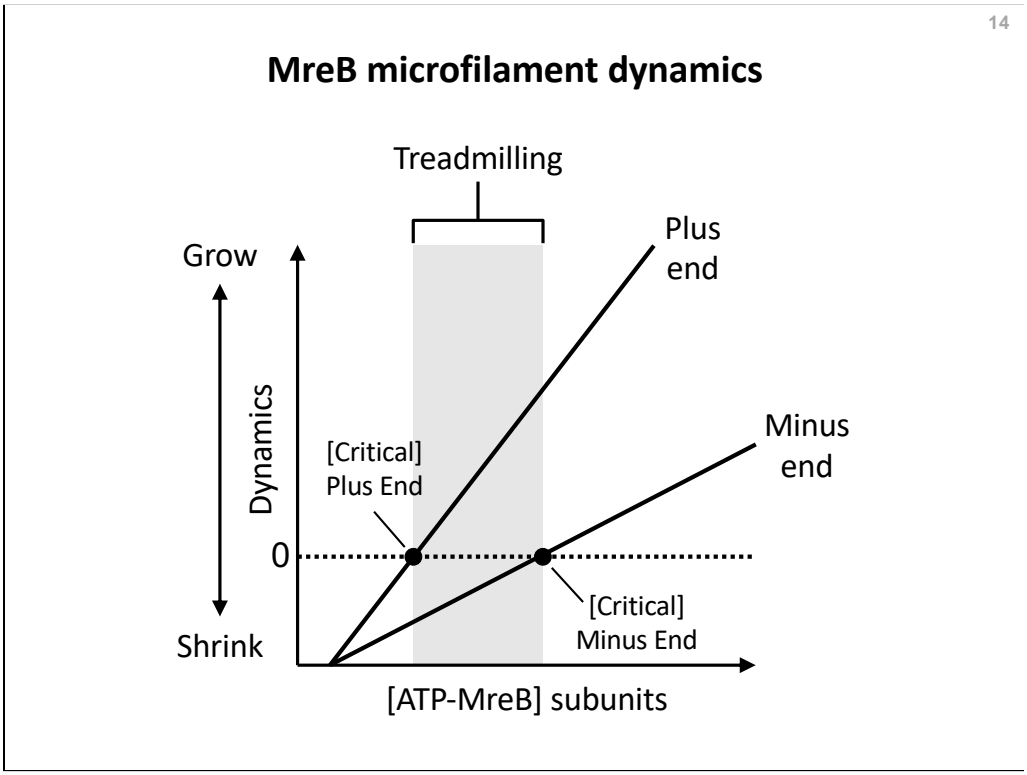

Source: http://www.ncbi.nlm.nih.gov/books/bv.fcgi?rid=mboc4.box.2958

C_cP is the critical concentration of ATP-MreB required for addition of new subunits to the **plus end** of a bacterial MreB (actin-like) filament.

C_cM is the critical concentration of ATP-MreB required for addition of new subunits to the **minus end** of a bacterial MreB (actin-like) filament.

Let's discuss the consequences of the different critical concentrations (C_c) at the plus and minus ends of MreB filaments.

ATP-MreB subunits add to the MreB filament. ADP-MreB subunits dissociate from the MreB filament *but only if they are exposed at the end of the filament*. MreB possesses an intrinsic ATPase activity so ATP-MreB subunits will self-convert to ADP-MreB subunits over time. The critical concentration of free ATP-MreB for addition to the plus end of an MreB filament (C_cP) is lower than the critical concentration of ATP-MreB for addition to the minus end of an MreB filament (C_cM). If the actual concentration of free ATP-MreB subunits is somewhere between C_cP and C_cM, then the plus end grows due to net addition of ATP-MreB subunits while the minus end shrinks due to net subtraction of ADP-MreB subunits, resulting in "treadmilling".

Let's put it another way. In the "treadmilling" range, addition of ATP-MreB subunits is faster than hydrolysis of ATP-MreB subunits (ATP-MreB –> ADP-MreB) at the plus end so the terminal subunits at the plus end are in the ATP-bound form, resulting in net growth and the MreB filament grows from the plus end. Conversely, addition of ATP-MreB subunits is slower than hydrolysis of ATP-MreB subunits (ATP-MreB –> ADP-MreB) at the minus end so the terminal subunits at the minus end are in the ADP-bound form and the MreB filament shrinks from the minus end.

In sum: in the "treadmilling" range of free ATP-MreB concentration, MreB filaments simultaneously grow from the plus end and shrink from the minus end.

15

At the concentration of free ATP-BALP subunits indicated by the red arrow, MreB microfilaments will:

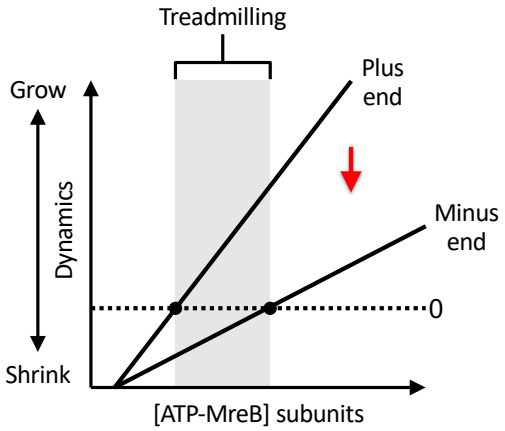

A. Grow from the plus end and the minus end.

B. Shrink from the plus end and the minus end.

C. Grow from the plus end and shrink from the minus end.

Answer: (A)

16

At the concentration of free ATP-BALP subunits indicated by the red arrow, MreB microfilaments will:

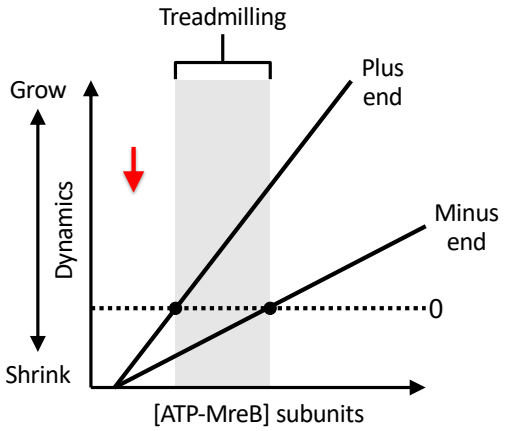

A. Grow from the plus end and the minus end.

B. Shrink from the plus end and the minus end.

C. Grow from the plus end and shrink from the minus end.

Answer: (B)

17

At the concentration of free ATP-BALP subunits indicated by the red arrow, MreB microfilaments will:

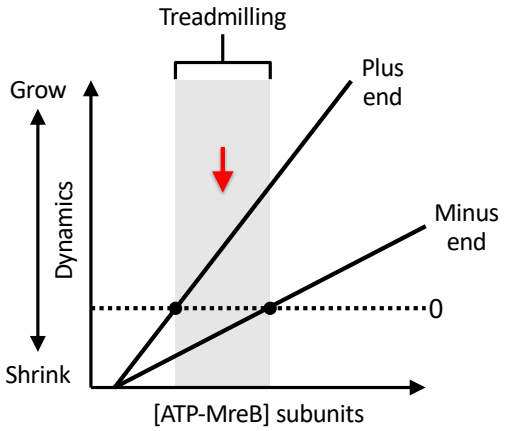

A. Grow from the plus end and the minus end.

B. Shrink from the plus end and the minus end.

C. Grow from the plus end and shrink from the minus end.

Answer: (C)

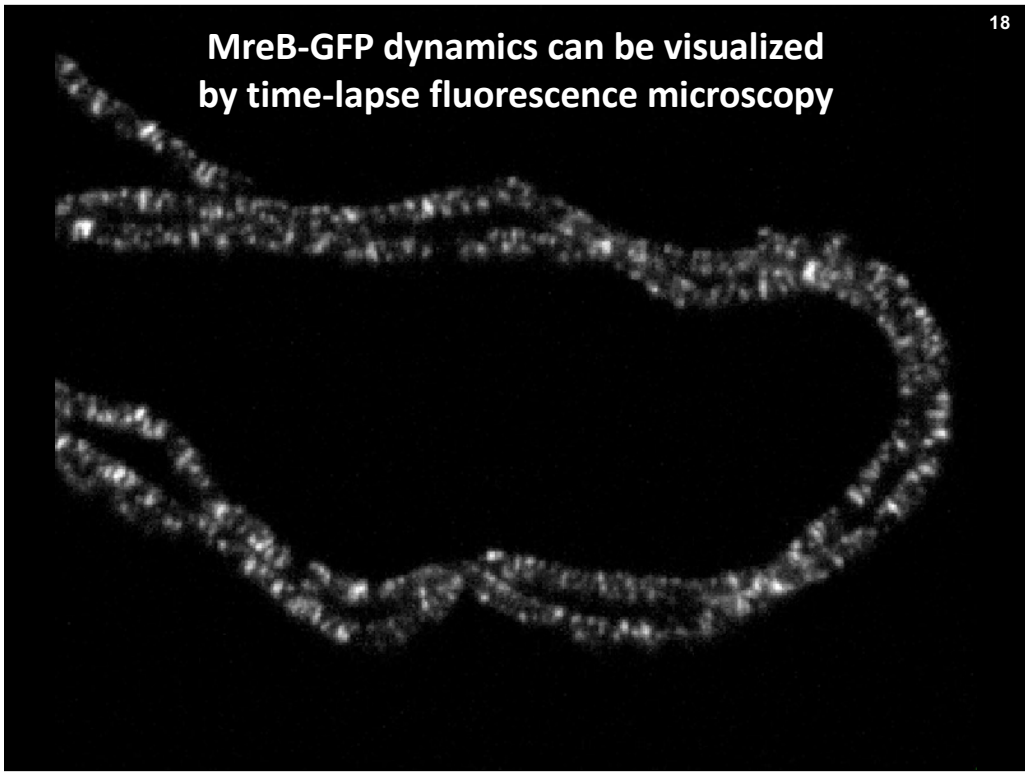

See: Movie_Slide18.mov posted on Moodle.

Source: Garner EC, Bernard R, Wang W, Zhuang X, Rudner X, Mitchison T (2011) Coupled, circumferential motions of the cell wall synthesis machinery and MreB filaments in *B. subtilis*. *Science* 333(6039): 222-225 PMID: 21636745.

Movie S1A. Time-lapse image series of *Bacillus subtilis* expressing MreB tagged with GFP. Frames are 5 seconds apart.

MreB filaments function as a scaffold for assembly of the cell-wall peptidoglycan synthesis complex ("elongasome")

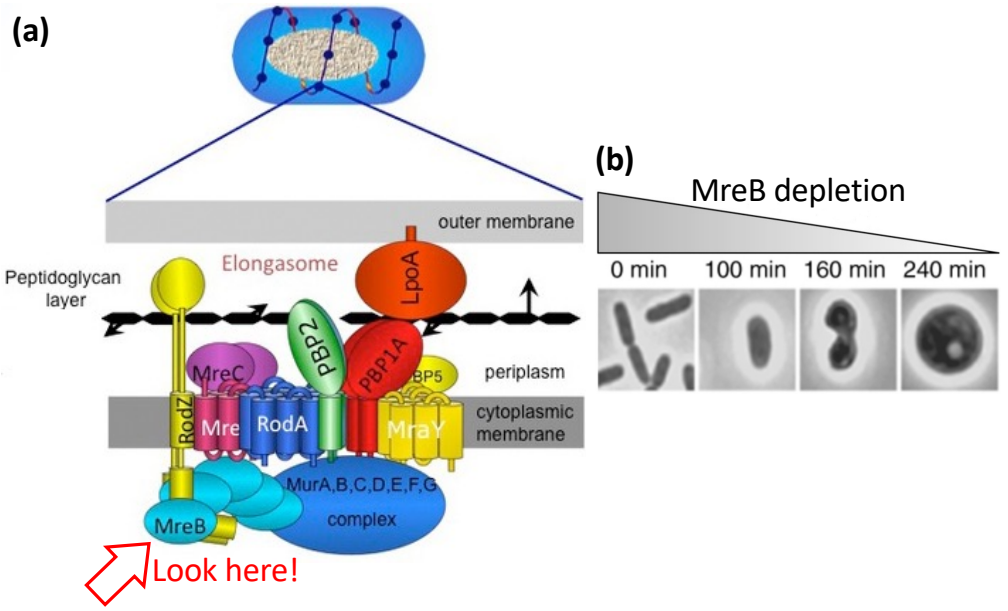

Source: Kruse T, Bork-Jensen J, Gerdes K (2005) The morphogenetic MreBCD proteins of *Escherichia coli* form an essential membrane-bound complex. *Mol Microbiol* 55(1): 78-89 PMID: 15612918.

(a) Schematic of protein-protein interactions within the MreB-MreC-MreD protein complex and interaction of MreB-MreC-MreD with periplasmic proteins involved in peptidoglycan synthesis. The MreB filament (cyan color; indicated by the red arrow) is located beneath the bacterial cytoplasmic membrane.

(b) Phase-contrast microscopy of bacteria (*Escherichia coli*) depleted for the MreB protein. Over time, there is a gradual transition from rod-shaped to spheroid morphology.

You do not need to memorize these proteins!!!

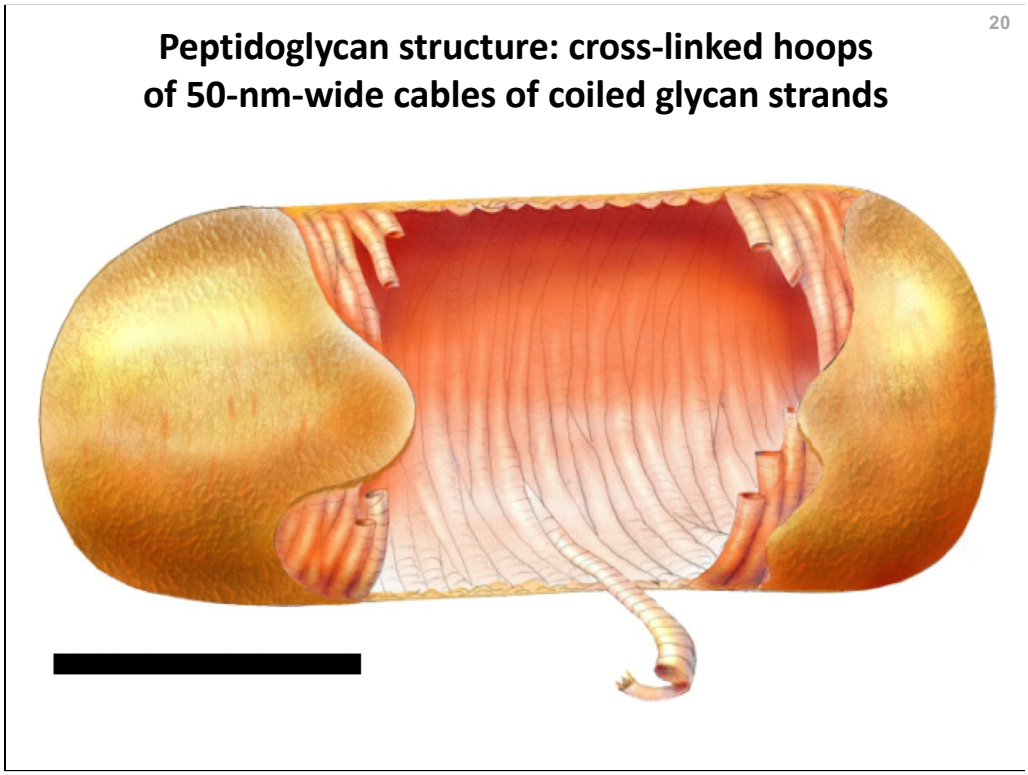

Source: Hayhurst EJ, Kailas L, Hobbs JK, Foster SJ (2008) Cell wall peptidoglycan architecture in *Bacillus subtilis*. *Proc Natl Acad Sci USA* 105(38): 14603-14608 PMID:18784364.

Figure 5. Model of *Bacillus subtilis* cell wall peptidoglycan architecture. Image is of a cell wall cylinder peptidoglycan architecture showing cable orientation with coiled substructure. Both cables and cross striations are shown. (Scale bar, 1 μm.)

Note that cables of peptidoglycan wrap around the short axis of the bacterial cell. This is presumably due to the fact that MreB filaments travel around the cell's short axis (slide 18), carrying complexes of peptidoglycan synthesis proteins (slide 19) along with them. Thus, peptidoglycan is synthesized as cables wrapping around the cell's short axis.

Working principle of atomic force microscopy (AFM) imaging

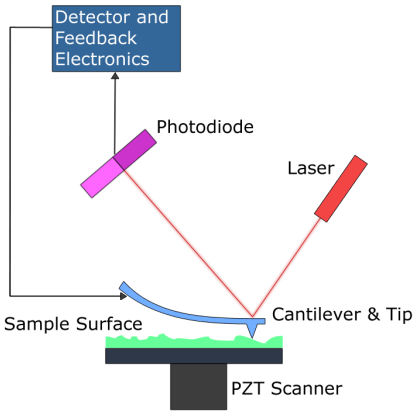

SOURCE: https://www.youtube.com/watch?v=uUdHanvrbjw

AFM, atomic force microscopy

Atomic force microscopy (AFM) can be used to image bacterial cells and probe their mechanical properties

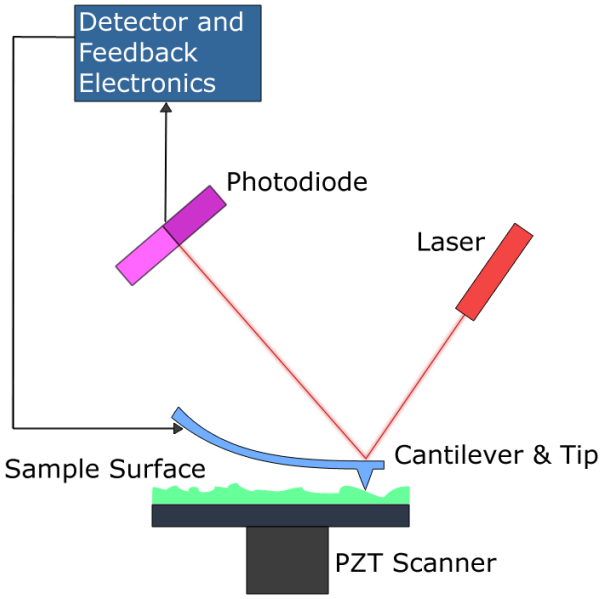

Hooke's Law: F = -*k* * D

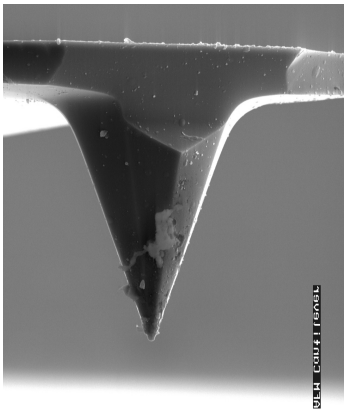

The atomic force microscope (AFM) is a high-resolution type of scanning probe microscopy with sub-nanometer resolution, which is more than 1,000 times better than the optical diffraction limit. The AFM is one of the foremost tools for imaging, measuring, and manipulating matter at the nanoscale. The information is gathered by "feeling" the surface with a mechanical probe. Piezoelectric elements that facilitate tiny but accurate and precise movements on electronic command enable the very precise scanning. The AFM consists of a cantilever with a sharp tip (probe) at its end that is used to scan the specimen surface. The cantilever typically has a tip radius of curvature on the order of nanometers. When the tip is brought into proximity of a sample surface, forces between the tip and the sample lead to a deflection of the cantilever according to **Hooke's law**. Deflection of the cantilever is measured using a laser spot reflected from the top surface of the cantilever onto an array of photodiodes. If the tip is scanned at a constant height, the tip could collide with the surface, causing damage, so a feedback mechanism is employed to adjust the tip-to-sample distance to maintain a constant force between the tip and the sample. The sample is mounted on a piezoelectric tube, which can move the sample in the Z direction to maintain a constant force and in the X and Y directions to scan the sample. The resulting map of the area s = f(X,Y) represents the sample's **topography**. The AFM can be operated in a number of modes, depending on the application. In general, imaging modes are divided into static (also called contact) modes and a variety of dynamic (or non-contact) modes where the cantilever is vibrated.

Hooke's law states that **F = -*k**d** where F is the restoring force exerted by the material in Newtons ($kg*m*s^{-2}$); d is the displacement of the spring from its equilibrium position (in m); k is the spring constant ($N*m^{-1}$ or $kg*s^{-2}$).

You should memorize the equation for Hooke's law and you should feel comfortable manipulating it. We will encounter Hooke's Law again later in this course.

The mesh-like ultrastructure of bacterial peptidoglycan revealed by AFM imaging

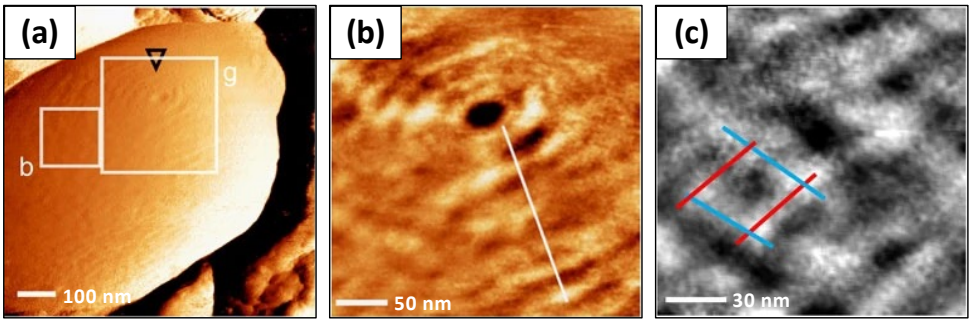

Source: Dover RS, Bitler A, Shimoni E, Trieu-Cuot P, Shai Y (2015) Multiparametric AFM reveals turgor-responsive net-like peptidoglycan architecture in live streptococci. *Nature Communications* 6: 7193 PMID: 26018339.

Figure 3. High-resolution AFM imaging reveals a nanoscale net-like surface architecture. (**a**) Low-magnification force-error images recorded in PBS using 1 nN peak force show circumferential surface bands (scale bars, 100 nm; the open triangle indicates the cell pole). (**b**) Height image, from a place marked in **a**, shows circumferential arrangement of bands around the cell pole (scale bar, 50 nm; height, 2.5 nm). (**c**) High-magnification height image shows a mesh-like surface topography (scale bars, 30 nm; height, 1.2 nm). Colored lines indicate holes formed by circumferential (blue) and connecting (red) bands. These might correspond to glycan strands (blue) and peptide crosslinks (red).

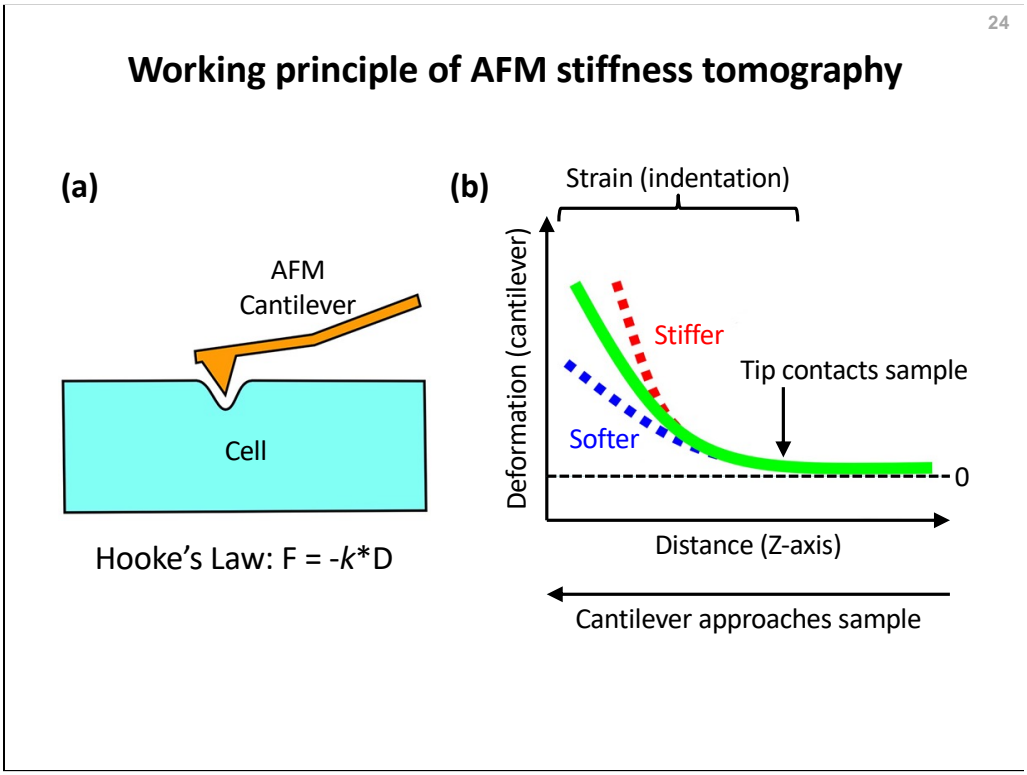

Source: Roduit C, Sekatski S, Dietler G, Catsicas S, Lafont F, Kasas S (2009) Stiffness tomography by atomic force microscopy. *Biophys J* 97(2): 674-677 PMID: 19619482.

Figure 1. "Deformation" means the bending of the cantilever as it pushes against an object. "Distance" means the Z-axis distance of the cantilever tip to the object. Deformation vs. Distance curves are recorded by indenting (pushing) the tip of the AFM cantilever into the sample **(a)** and by plotting the deformation of the cantilever as a function of the height on the Z-axis **(b)**.

Imagine that the green curve in **(b)** represents the recording for a "normal" bacterial cell. Conditions that produce a "stiffer" cell, e.g. suspending the cell in a hypotonic medium, will produce a steeper curve (dashed red line). Conditions that produce a "softer" cell, e.g. suspending the cell in a hypertonic medium, will produce a less-steep curve (dashed blue line).

Deformation vs. Distance curves can be converted to Force vs. Distance curves using Hooke's Law: $F = -k*D$, where F is force (in newtons), D is distance (in meters), and k is the cantilever's spring constant in newtons per meter. Typical k values for an AFM cantilever are about 0.5 to 1.0 $N*m^{-1}$ but cantilevers can be "tuned" to the desired stiffness for measuring very stiff or very soft samples.

Force vs. Distance curves can be converted to Stress vs. Strain curves using the known surface area of the AFM cantilever tip. Stress equals Force divided by Surface Area (same units as Pressure). Strain (indentation of the cell) is proportional to the Deformation of the cantilever tip.

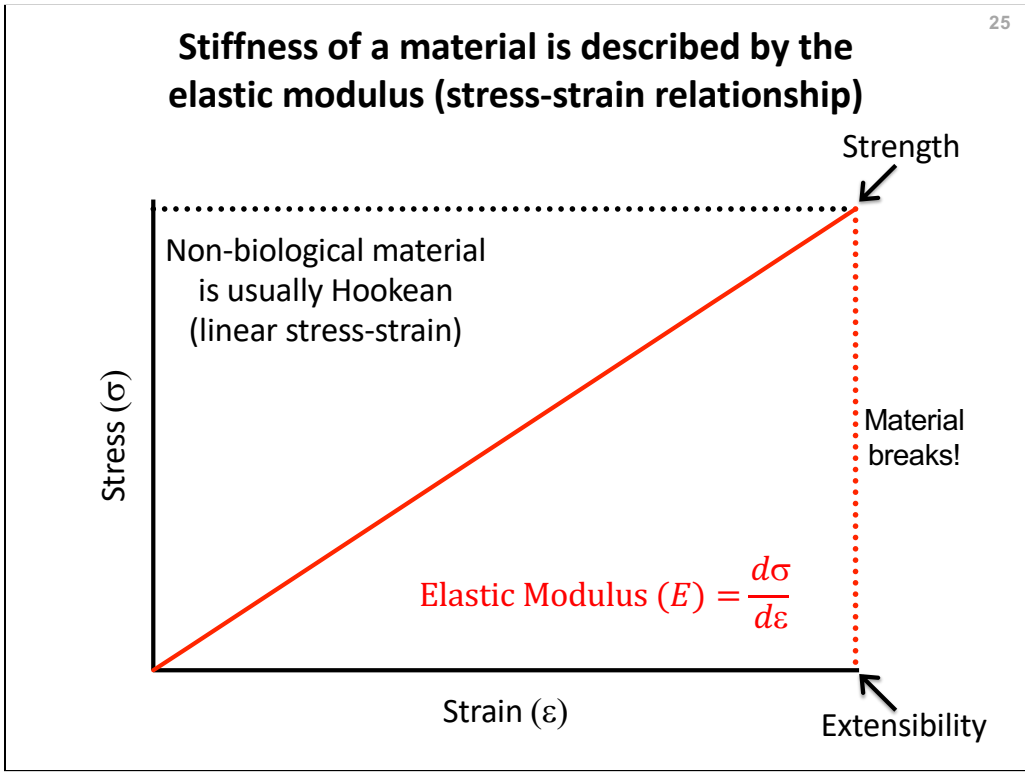

Source: *Comparative Biomechanics: Life's Physical World [2nd Edition]*, by Vogel S, published by Princeton University Press, Princeton, NJ (p. 297) © 2013.

Figure 15.3. A graph of **Stress** (y-axis) versus **Strain** (x-axis) showing five of the six material properties that such a graph can display: **Strength**, **Extensibility**, **Elastic Modulus** (a.k.a. Young's Modulus), **Tangent Modulus** (see slide 26), and **Toughness**. Note that **Compressive Strength** is not shown.

Stress* (σ) is defined as: Force/Area = Pa = N * m^{-2} = kg * m^{-1} * s^{-2}

Note that Stress and Pressure are expressed in the same units: Pa = N * m^{-2} = kg * m^{-1} * s^{-2}

Strain* (ε) is defined as: (Stretched Length – Unstretched Length)/(Unstretched Length)

Note that Strain is dimensionless.

Strength* of a material is defined as the stress that the material can withstand before breaking.

Extensibility* of a material is defined as the strain that it can withstand before breaking.

Elastic modulus* (*E*) or elasticity of a material is defined as the slope of the stress/strain curve = dσ/dε

Toughness* of a material is defined as the area under the stress-strain curve up to the material's breaking point.

Note that the stiffness of peptidoglycan is similar to rubber, about 25 MPa (PMID: 18355161).

***You should memorize these terms and their mathematical definitions!**

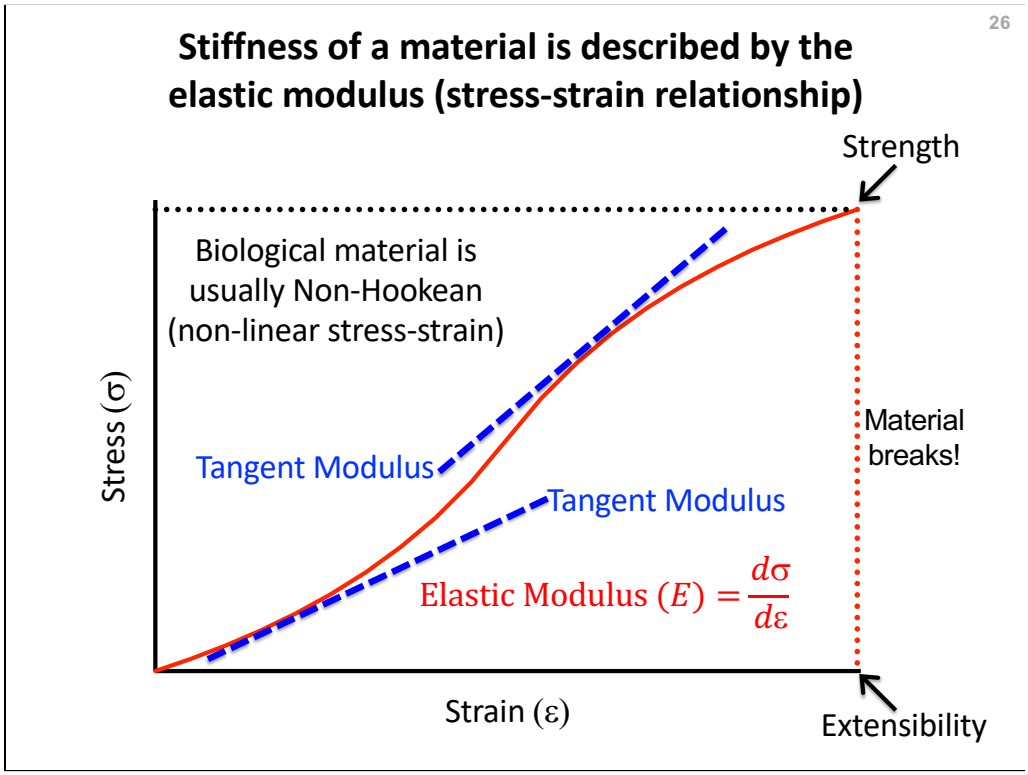

Source: *Comparative Biomechanics: Life's Physical World [2nd Edition]*, by Vogel S, published by Princeton University Press, Princeton, NJ (p. 297) © 2013.

Figure 15.3. A graph of **Stress** (y-axis) versus **Strain** (x-axis) showing five of the six material properties that such a graph can display: **Strength**, **Extensibility**, **Elastic Modulus** (a.k.a. Young's Modulus), **Tangent Modulus** (see slide 26), and **Toughness**. Note that **Compressive Strength** is not shown.

Stress* (σ) is defined as: Force/Area = Pa = N * m^{-2} = kg * m^{-1} * s^{-2}

Note that Stress and Pressure are expressed in the same units: Pa = N * m^{-2} = kg * m^{-1} * s^{-2}

Strain* (ε) is defined as: (Stretched Length – Unstretched Length)/(Unstretched Length)

Note that Strain is dimensionless.

Strength* of a material is defined as the stress that the material can withstand before breaking.

Extensibility* of a material is defined as the strain that it can withstand before breaking.

Elastic modulus* (*E*) or elasticity of a material is defined as the slope of the stress/strain curve = dσ/dε

Toughness* of a material is defined as the area under the stress-strain curve up to the material's breaking point.

Note that the stiffness of peptidoglycan is similar to rubber, about 25 MPa (PMID: 18355161).

***You should memorize these terms and their mathematical definitions!**

27

Which cell is stiffer?

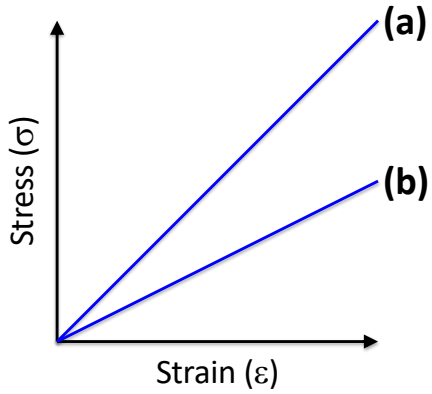

A. Cell (a).

B. Cell (b).

C. Cells (a) and (b) are equally stiff.

D. Impossible to tell from this graph.

Answer: (A)

28

Which cell is stronger?

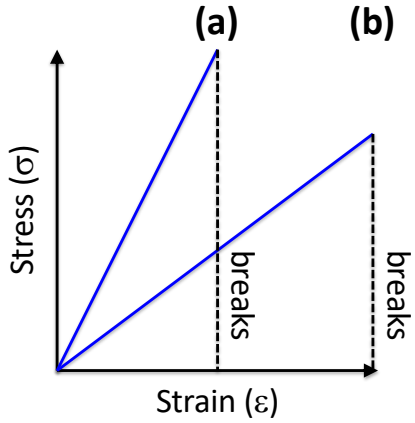

A. Cell (a).

B. Cell (b).

C. Cells (a) and (b) are equally strong.

D. Impossible to tell from this graph.

Answer: (A)

29

Which cell is more extensible?

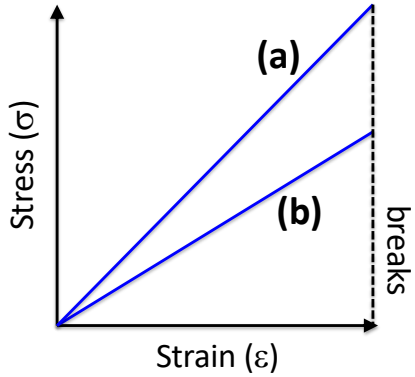

A. Cell (a).

B. Cell (b).

C. Cells (a) and (b) are equally extensible.

D. Impossible to tell from this graph.

Answer: (C)

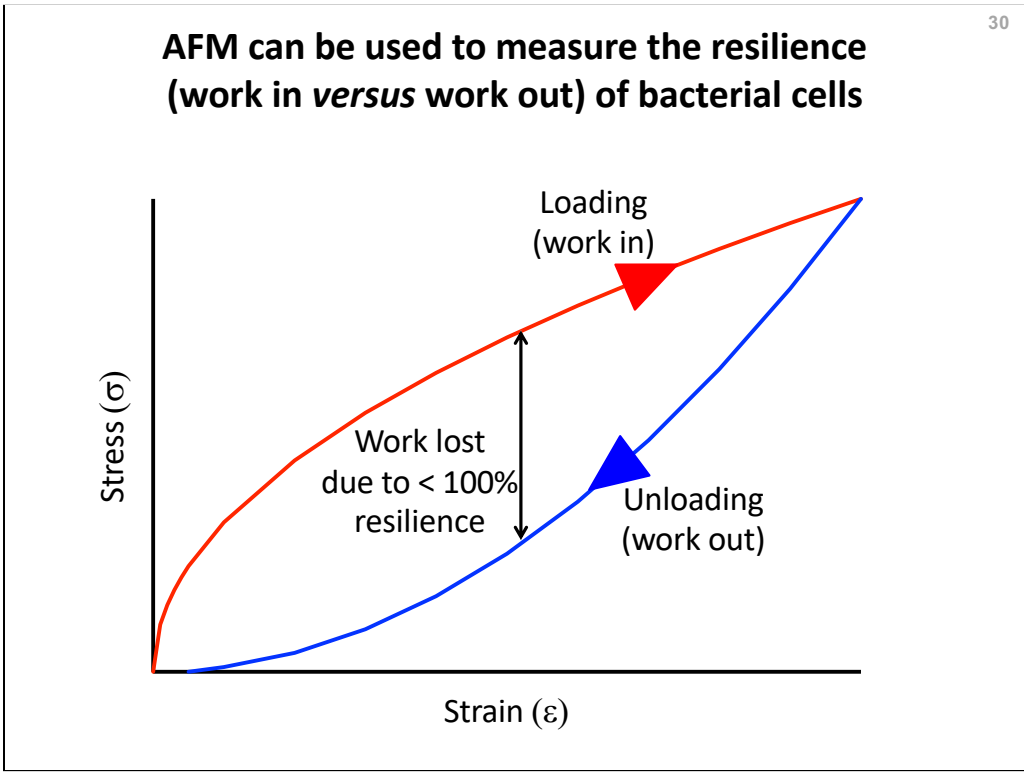

Work is defined as (force) * (distance) = N * m = Joules.

Remember: 1 joule is equal to the amount of work done when a force of 1 newton displaces a mass through a distance of 1 meter in the direction of that force. Units: N * m = kg * m^2 * s^{-2}.

31

Which cell is more resilient?

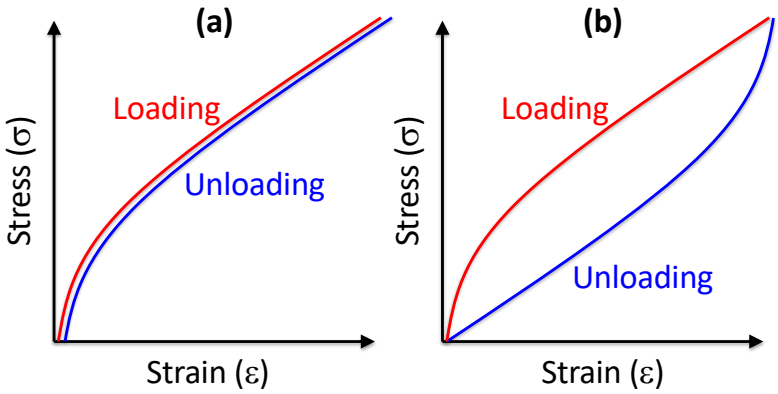

A. Cell (a).

B. Cell (b).

C. Cells (a) and (b) are equally resilient.

D. Impossible to tell from this graph.

Answer: (A)

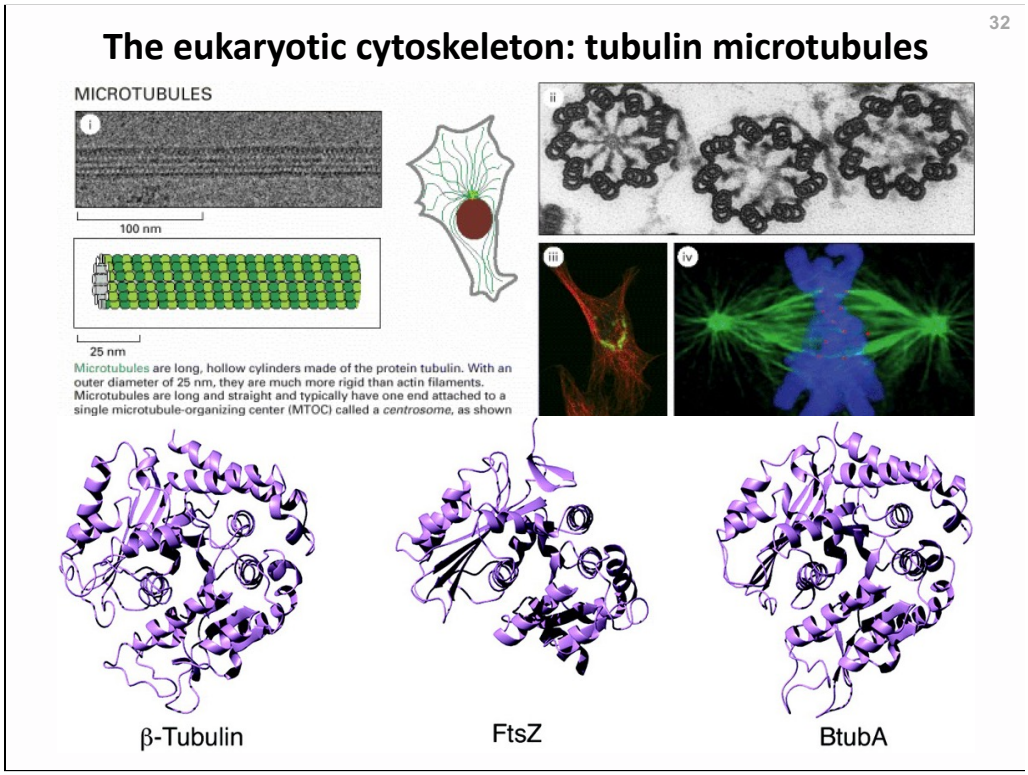

Source: http://www.ncbi.nlm.nih.gov/books/bv.fcgi?rid=mboc4.box.2958

Figure 16-1. The three major types of protein that form the cytoskeleton: tubulin microtubules.

Source: Shih YL, Rothfield L (2006) The bacterial cytoskeleton. *Microbiol Mol Biol Rev* 70(3): 729-754 PMID: 16959967.

Figure 1. Structural comparison of eukaryotic tubulin and prokaryotic tubulin-like cytoskeletal proteins. **Left:** Eukaryotic beta-tubulin from *Bos taurus*. **Middle:** Prokaryotic tubulin-like protein (FtsZ) from *Methanococcus jannaschii* (Archaea). **Right:** Prokaryotic tubulin-like protein (BtubA) from *Prosthecobacter dejongeii* (Bacteria).

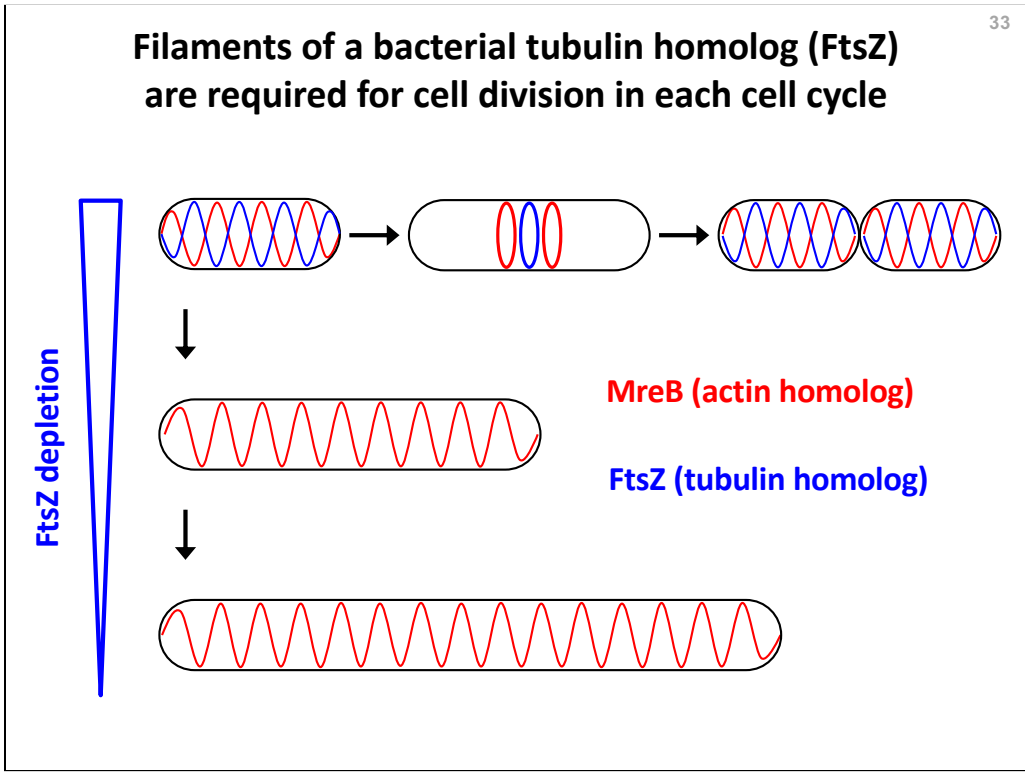

Source: Margolin M (2009) Sculpting the bacterial cell. *Curr Biol* 19(17): R812-R822 PMID: 19906583.

Figure 2. Roles for the actin-like MreB protein (red) and tubulin-like FtsZ protein (blue) in shaping bacterial cells.

Top row. During normal bacterial cell growth and division, FtsZ and MreB localize as hoops or helices wrapped around the short axis of the cell. When cells prepare to divide these helices collapse into a single FtsZ ring flanked by two MreB rings. After division, the FtsZ and MreB rings return to the original configuration.

Middle row. Depletion of FtsZ (indicated by the inverted blue triangle) disrupts the FtsZ cytoskeleton and causes cells to grow (elongate) without dividing.

Bottom row. FtsZ-depleted cells continue to grow, forming long cylindrical filaments containing extended helices of MreB over time. Although FtsZ-depleted cells continue to grow, they are not very "happy" (i.e., growth is slow compared to normal rod-shaped cells and elongated cells eventually undergo death and lysis).

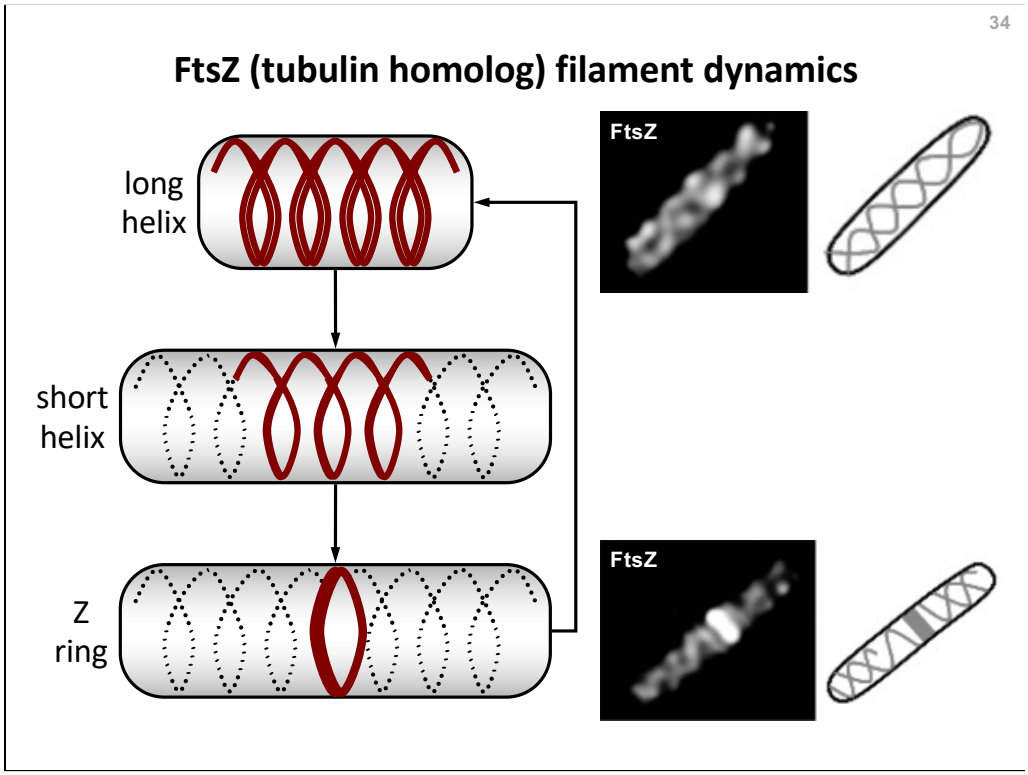

Source: Peters PC, Migocki MD, Thoni C, Harry EJ (2007) A new assembly pathway for the cytogenetic Z ring from a dynamic helical structure in vegetatively growing cells of *Bacillus subtilis*. *Mol Microbiol* 64(2): 487-499 PMID: 17493130.

Figure 9. Model for the pathway of FtsZ polymerization during the cell cycle, leading to establishment of the FtsZ ring at the division site at midcell. Solid lines indicate the dominant location and pattern of FtsZ at the different stages of the cell cycle, with dotted lines denoting a lower concentration of FtsZ that comprises a permanent cytoskeletal coil.

In the fluorescence microcopy images (insets), FtsZ was tagged with GFP.

35

The bacterial FtsZ ring functions as a scaffold for assembly of the cell division complex ("divisome")

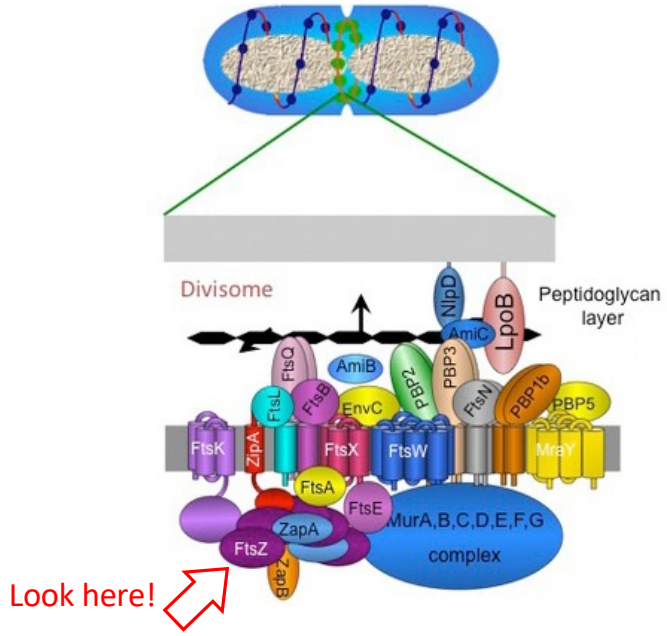

Source: Kruse T, Bork-Jensen J, Gerdes K (2005) The morphogenetic MreBCD proteins of *Escherichia coli* form an essential membrane-bound complex. *Mol Microbiol* 55(1): 78-89 PMID: 15612918.

You do not need to memorize these proteins!!!

MinD is a highly conserved cytoskeletal element present in Archaea and Bacteria but not Eukarya

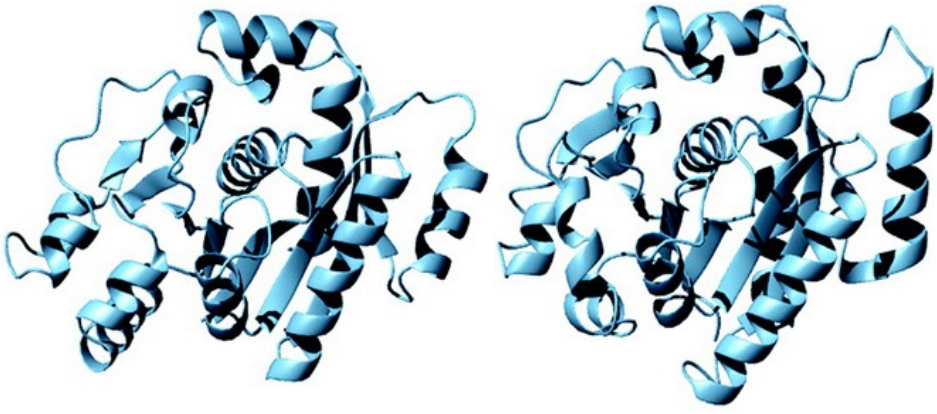

A. fulgidus **(Archaea)**

T. thermophilus **(Bacteria)**

Source: Shih YL, Rothfield L (2006) The bacterial cytoskeleton. *Microbiol Mol Biol Rev* 70(3): 729-754 PMID:16959967.

Figure 1. Structural comparison of prokaryotic cytoskeletal proteins.

Left: *Archaeoglobus fulgidus* MinD. *Archaeoglobus fulgidus* is a sulphur-metabolizing archaeon.

Right: *Thermus thermophilus* MinD. *T. thermophilus* is a Gram-negative bacterium.

Archaea and Bacteria comprise two of the three Domains of life (the third Domain is Eukarya). The Archaea and Bacteria diverged from each other (evolutionarily) about 3.7 billion years ago. Thus, the striking conservation of three-dimensional structure between MinD in Archaea and MinD in Bacteria is particularly noteworthy, especially when one considers that MinD is not present in Eukarya.

FtsZ ring localization is driven by MinCD dynamics

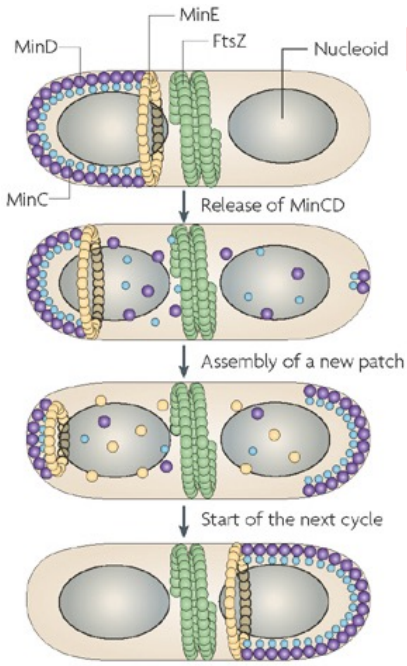

MinC inhibits FtsZ polymerization

MinC binds to MinD-ATP

MinCD-ATP binds to cell poles

MinCD-ATP makes filaments

MinE binds to MinCD-ATP

MinE stimulates MinD ATPase

MinCD-ATP > MinCD-ADP

MinCD-ADP disassembles

Source: Thanbichler M, Shapiro L (2008) Getting organized – how bacterial cells move proteins and DNA. *Nat Rev Microbiol* 6(1): 28-40 PMID: 18059290.

Source: Thanbichler M, Shapiro L (2006) MipZ, a spatial regulator coordinating chromosome segregation with cell division in *Caulobacter*. *Cell* 126(1): 147-162 PMID:16839883.

Figure 5. Positioning of the cell division plane. In *Escherichia coli*, assembly of the FtsZ ring is restricted to the mid-cell by the MinE-driven pole-to-pole oscillation of MinCD, a complex of the MinC and MinD proteins that inhibits polymerization of FtsZ. Over time, the only place in the cell where MinCD never accumulates to high levels is the middle of the cell. Thus, FtsZ polymerization to form the Z-ring is inhibited by MinCD at both cell poles but not at the cell center. Consequently, formation of the Z-ring is restricted to the middle of the cell.

Stochastic simulation of MinD pole-to-pole oscillations

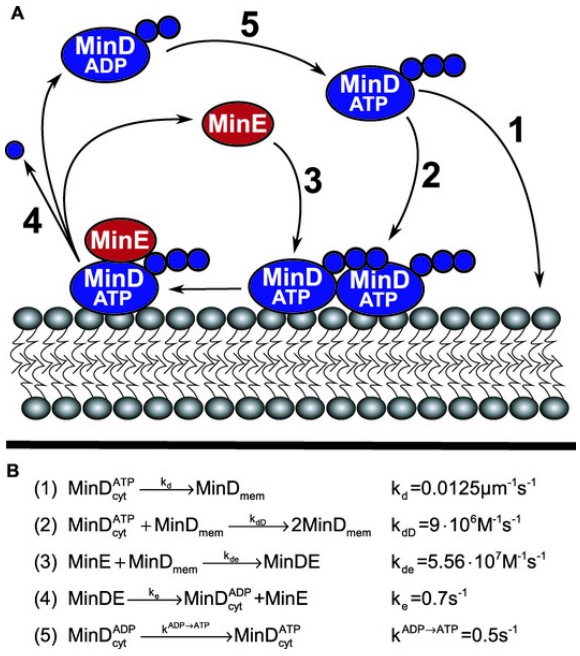

Source: Fange D, Elf J (2006) Noise-induced Min phenotypes in *Escherichia coli*. *PLoS Comput Biol* 2(6): e80 PMID: 16846247.

Figure 2. Schematic of the Min system **(A)** and the corresponding reaction scheme and rate constants **(B)**. The diffusion constant for proteins in the cytoplasm is 2.5 × 10^{-8} cm^2s^{-1} and in the membrane, 1 × 10^{-10} cm^2s^{-1}.

You do not need to memorize these equations or the biochemical parameters! The purpose of this slide is just to illustrate that the complex and self-organizing behavior shown on the next slide can be modeled using a small number of simple equations and experimentally measured biochemical parameters. This is less common in biology than you might think…

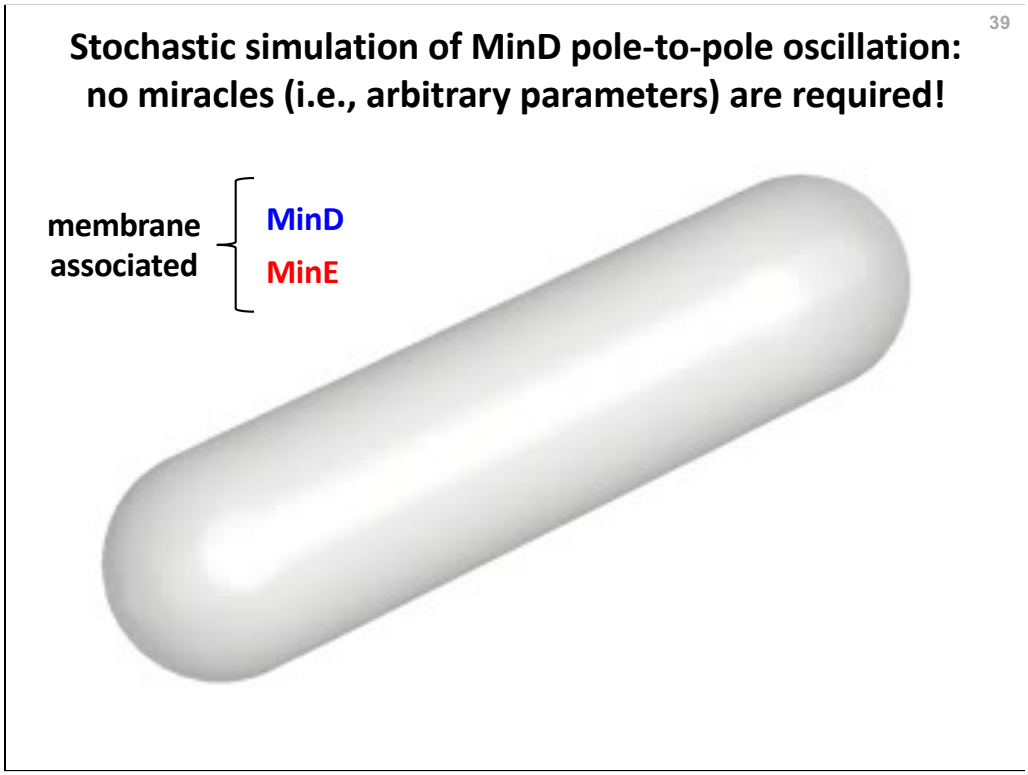

Source: Fange D, Elf J (2006) Noise-induced Min phenotypes in *Escherichia coli*. *PLoS Comput Biol* 2(6): e80 PMID: 16846247.

Video S1. Stochastic simulation of a wild-type cell geometry of length 4.5 µm. Initial conditions as described in the text. Membrane-bound MinD is shown in blue. MinD in complex with MinE on the membrane is shown in red. Although not shown here, remember: MinC (which inhibits FtsZ polymerization) binds tightly to MinD-ATP, so wherever there is MinD-ATP there is also MinC.

See: Movie_Slide39.mov posted on Moodle.

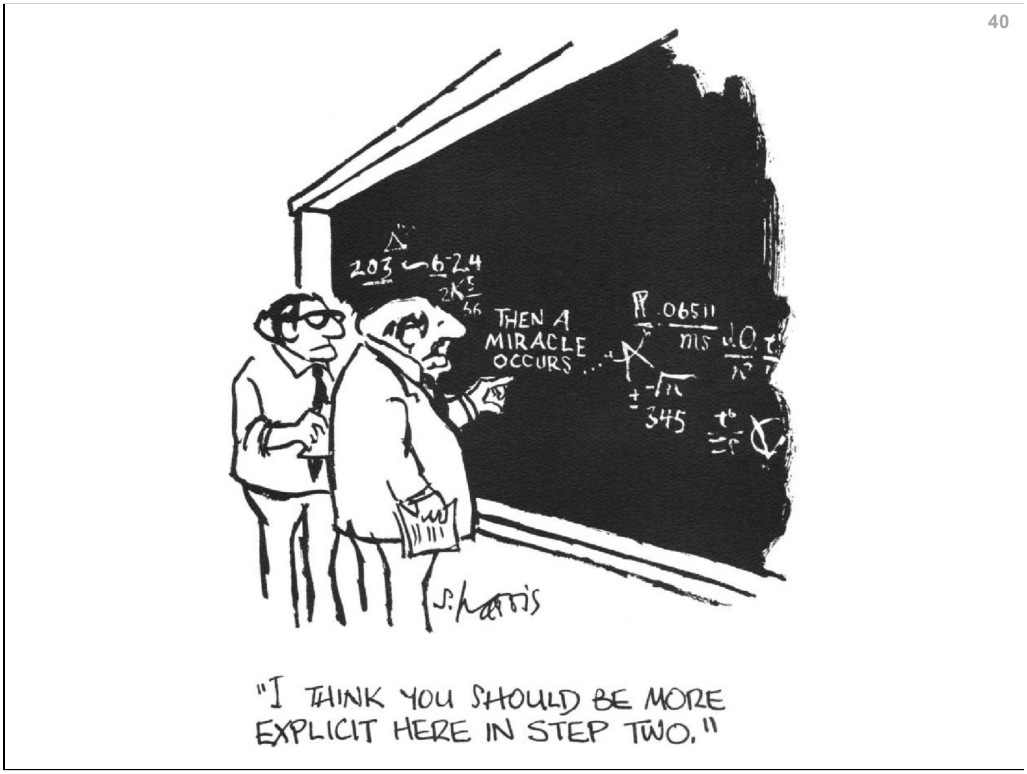

Computational models of complex biological phenomena often require “miracles” (also known as “arbitrary parameters”) to reproduce the desired behavior. The remarkable pole-to-pole oscillations of the MinCD and MinE proteins (see Slide 39) can be accurately reproduced using just a few experimentally-measured biochemical parameters and simple equations (see Slide 38).

What’s the problem with using arbitrary parameters in computational models? The problem is memorably captured in this amusing conversation between Freeman Dyson and Enrico Fermi, as related by Dyson:

When I arrived in Fermi's office, I handed the graphs to Fermi, but he hardly glanced at them. He invited me to sit down, and asked me in a friendly way about the health of my wife and our new-born baby son, now fifty years old. Then he delivered his verdict in a quiet, even voice. "There are two ways of doing calculations in theoretical physics", he said. "One way, and this is the way I prefer, is to have a clear physical picture of the process that you are calculating. The other way is to have a precise and self-consistent mathematical formalism. You have neither." I was slightly stunned, but ventured to ask him why he did not consider the pseudoscalar meson theory to be a self-consistent mathematical formalism. He replied, "Quantum electrodynamics is a good theory because the forces are weak, and when the formalism is ambiguous we have a clear physical picture to guide us. With the pseudoscalar meson theory there is no physical picture, and the forces are so strong that nothing converges. To reach your calculated results, you had to introduce arbitrary cut-off procedures that are not based either on solid physics or on solid mathematics."

In desperation I asked Fermi whether he was not impressed by the agreement between our calculated numbers and his measured numbers. He replied, "How many arbitrary parameters did you use for your calculations?" I thought for a moment about our cut-off procedures and said, "Four." He said, "I remember my friend Johnny von Neumann used to say, with four parameters I can fit an elephant, and with five I can make him wiggle his trunk." With that, the conversation was over. I thanked Fermi for his time and trouble, and sadly took the next bus back to Ithaca to tell the bad news to the students. Because it was important for the students to have their names on a published paper, we did not abandon our calculations immediately. We finished them and wrote a long paper that was duly published in the Physical Review with all our names on it. Then we dispersed to find other lines of work. I escaped to Berkeley, California, to start a new career in condensed-matter physics.

SOURCE: *Turning Points – A Meeting with Enrico Fermi* (http://lilith.fisica.ufmg.br/~dsoares/fdyson.htm)

The eukaryotic cytoskeleton: intermediate filaments

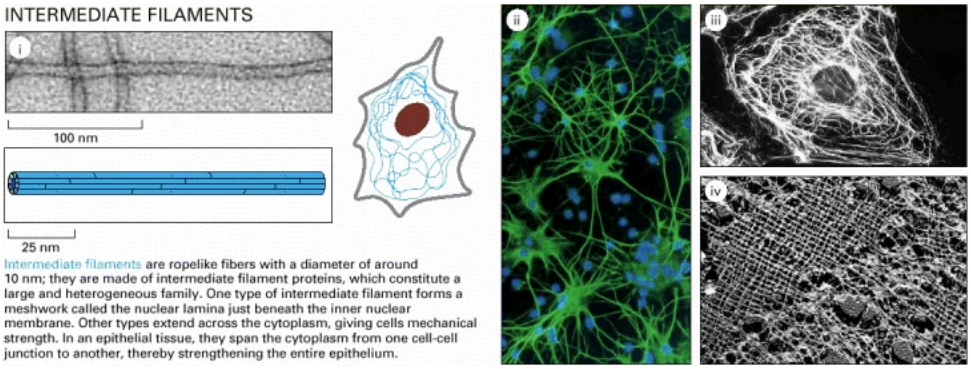

Source: http://www.ncbi.nlm.nih.gov/books/bv.fcgi?rid=mboc4.box.2958

Figure 16-1. The three major types of protein that form the eukaryotic cytoskeleton: actin filaments, tubulin microtubules, and intermediate filaments.

Intermediate filaments form coiled-coil structures

Amphipathic alpha helix

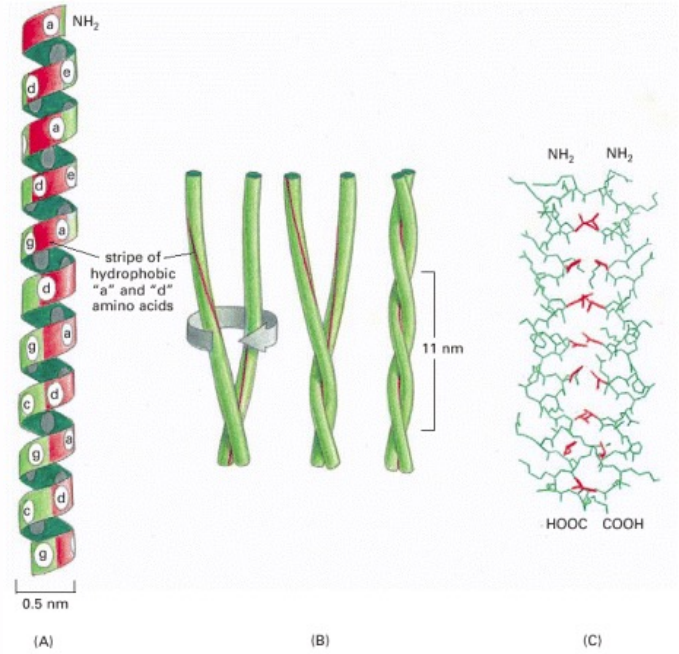

Source: http://www.ncbi.nlm.nih.gov/books/bv.fcgi?highlight=coiled-coil&rid=mboc4.figgrp.405

Figure 3-11. The structure of a coiled-coil. **(A)** A single alpha helix, with successive amino acid side chains labeled in a sevenfold sequence, "abcdefg" (from bottom to top). Amino acids "a" and "d" in such a sequence lie close together on the cylinder surface, forming a "stripe" (*red*) that winds slowly around the alpha helix. Proteins that form coiled-coils typically have nonpolar amino acids at positions "a" and "d". Consequently, as shown in **(B)**, the two alpha helices can wrap around each other with the nonpolar side chains of one alpha helix interacting with the nonpolar side chains of the other, while the more hydrophilic amino acid side chains are left exposed to the aqueous environment. **(C)** The atomic structure of a coiled-coil determined by x-ray crystallography. The *red* side chains are nonpolar. Note that the two alpha-helices are arrange in a parallel fashion, with N- and C- termini on the same end of the coiled-coil structure.

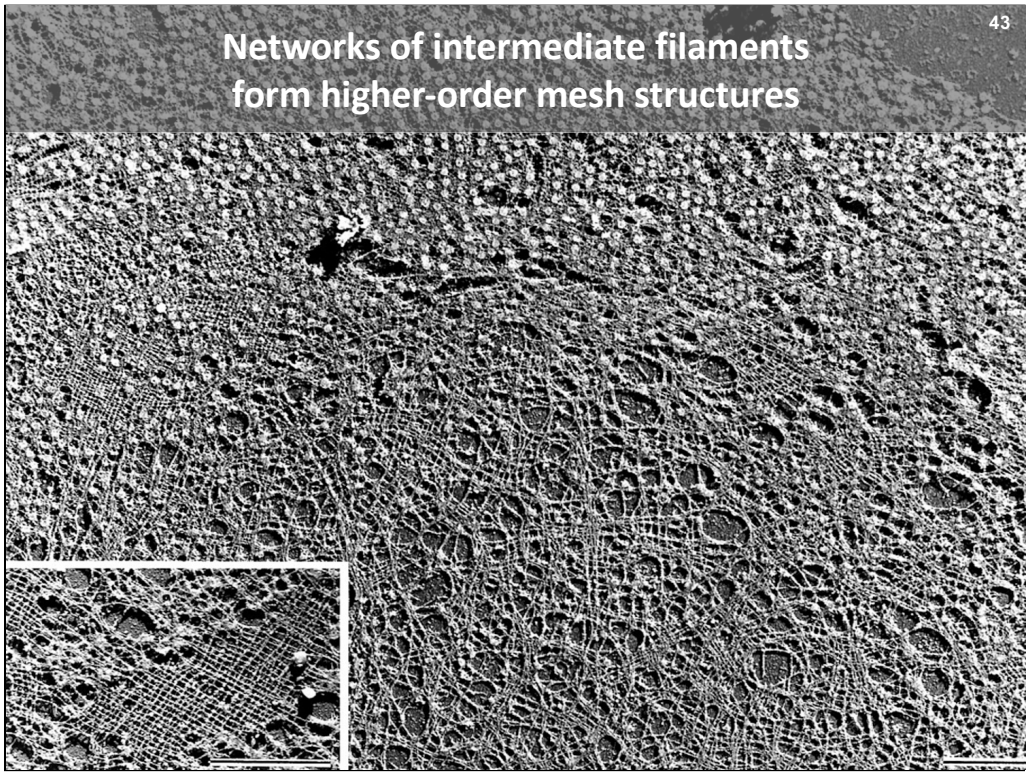

Source: Stuurman N., Heins S., Aebi U. (1998) Nuclear lamins: their structure, assembly, and interactions. *J. Struct. Biol.* 122(1-2): 42-66 PMID: 9724605.

Figure 2. This electron micrograph illustrates the mesh-like structure of an intermediate filament network (specifically, the "nuclear lamina" in frog eggs). The inset shows a higher-magnification view of a particularly well-preserved area of the near-tetragonal lamina mesh-like structure, which resembles burlap ("toile de jute" in French). Bars, 1 µm.

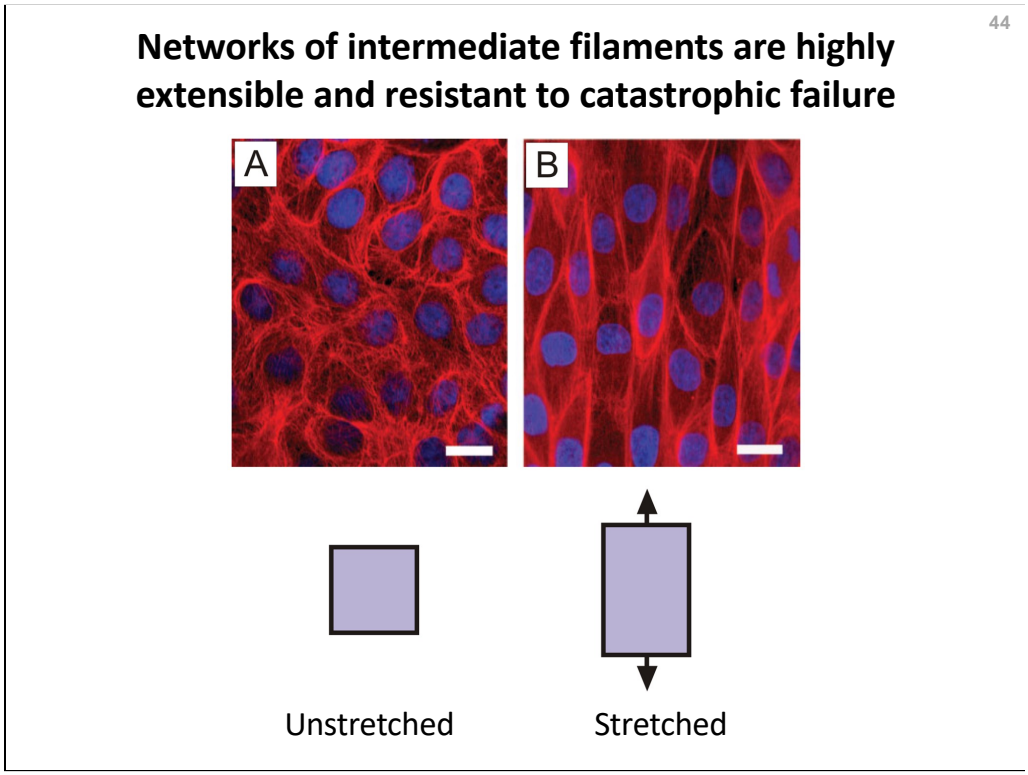

Source: Ackbarow T., Sen D., Thaulow C., Buehler M.J. (2009) Alpha-helical protein networks are self-protective and flaw-tolerant. *PLoS One* 4(6): e6015 PMID:19547709.

Figure 2. Effect of large uniaxial stretch on the intermediate filament network in MDCK cells, illustrating the ability of intermediate filament network to undergo very large deformation without catastrophic failure. The cells were grown on collagen-coated silastic membranes and stretched using a custom cell stretcher that was mounted on a confocal microscope. Cells were fixed and stained for immunofluorescence (red = keratin intermediate filaments, blue = DNA). Subplot A: Control cells were processed on a relaxed silastic membrane. Subplot B: Stretched cells were fixed, stained and imaged on membranes that were held in the stretched state. The approximate uniaxial strain in stretched cells is 75%. Scale bar is approximately 25 µm. Images reprinted from reference [46], Biomechanical properties of intermediate filaments: from tissues to single filaments and back, Vol. 29, No. 1, 2007, pp. 26-35, copyright © 2007 John Wiley & Sons, Inc.

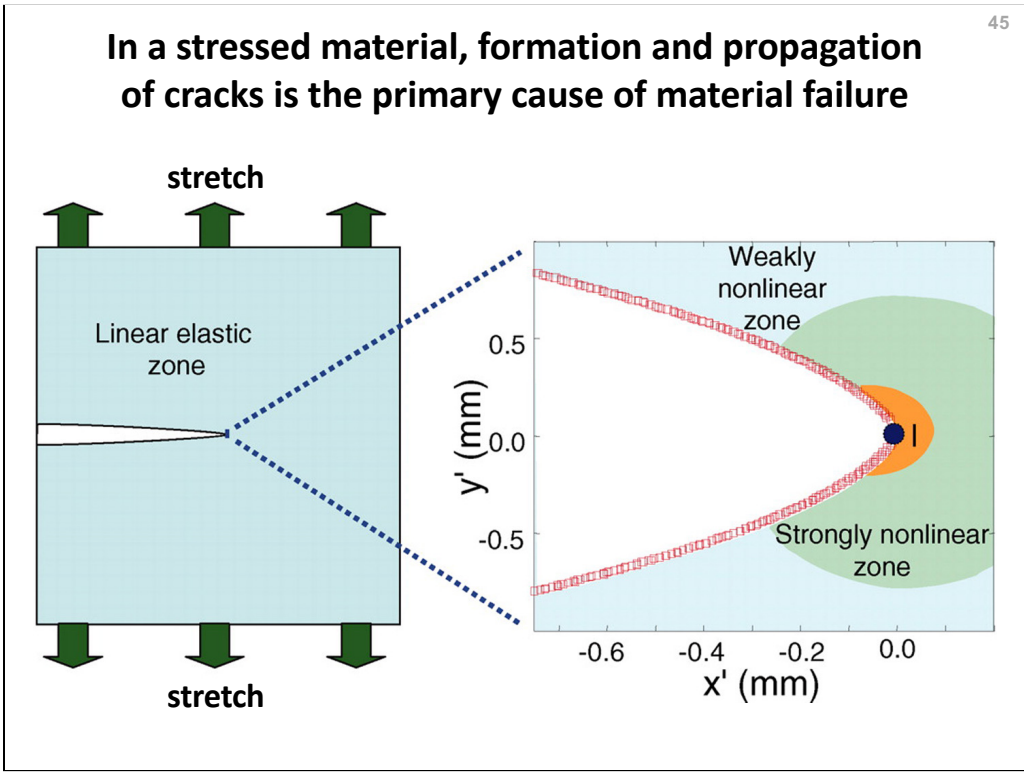

SOURCE: Livne A, Bouchbinder E, Svetlizky I, Fineberg J (2010) The near-tip fields of fast cracks. *Science* 327(5971): 1359-1363 PMID:20223982.

Figure 4. Addressing the different elastic zones in the vicinity of a crack tip provides a full description of the material deformation down to the dissipation scales. The figure shows a schematic sketch of the different elastic regions surrounding a crack. Energy and stresses are transmitted from the large scales, where material deformation is described by linear elasticity (left), through a hierarchy of nonlinear elastic regions (right) until dissipated by plastic deformation and fracture at the smallest scales (orange circle).

If you pull on a piece of paper in the direction shown, will it tear in the direction shown in (a) or (b)?

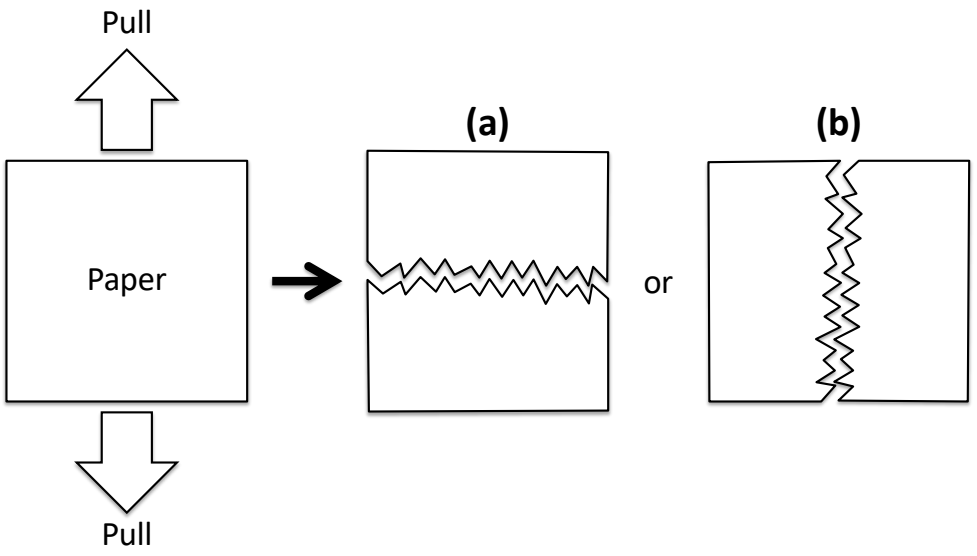

Answer: (a)

Can you explain why?

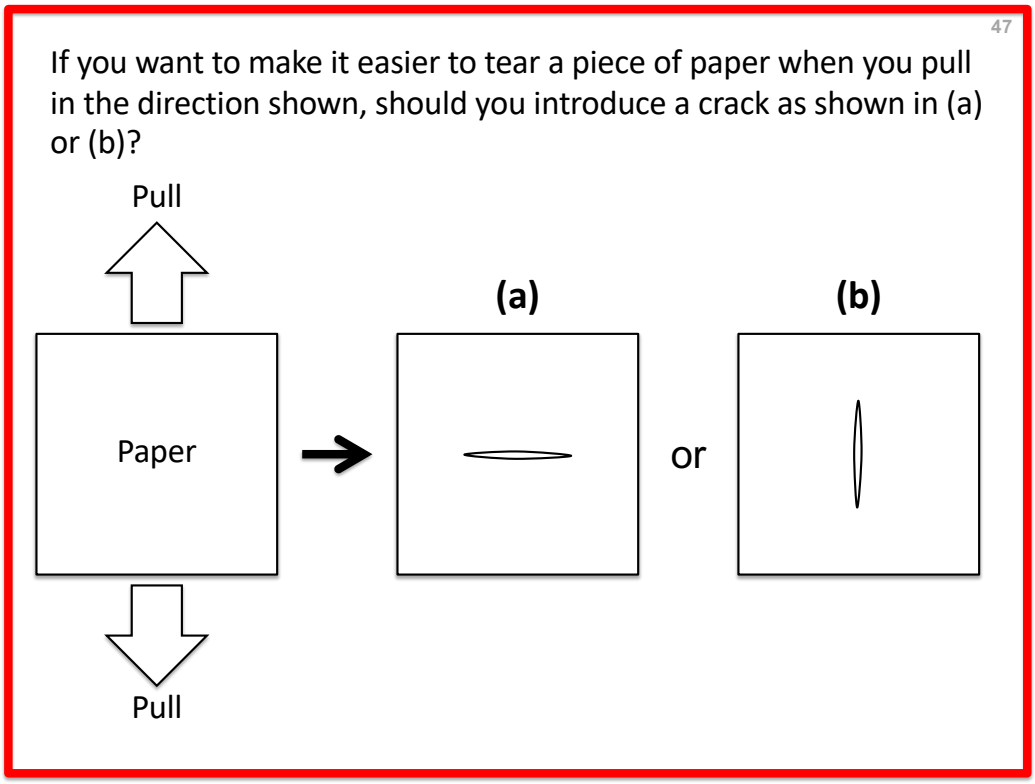

Answer: (a)

Can you explain why?

I encourage you to demonstrate this principle to yourself with a piece of paper and scissors. First try to tear the paper by pulling on it as shown in the diagram. Not so easy, right? Now introduce a "crack" by making a small incision in the paper with scissors as shown in (b) then pull on the paper as shown in the diagram. Still not so easy, right? Now turn the "cracked" paper by 90 degrees so the orientation of the crack relative to the pulling direction is as shown in (a) and try again. What a difference! You have just demonstrated why crack propagation is the primary cause of material failure in a stressed body, as stated in slide 45.

Intermediate filament networks are extensible and crack-resistant (because the crack tips are blunted)

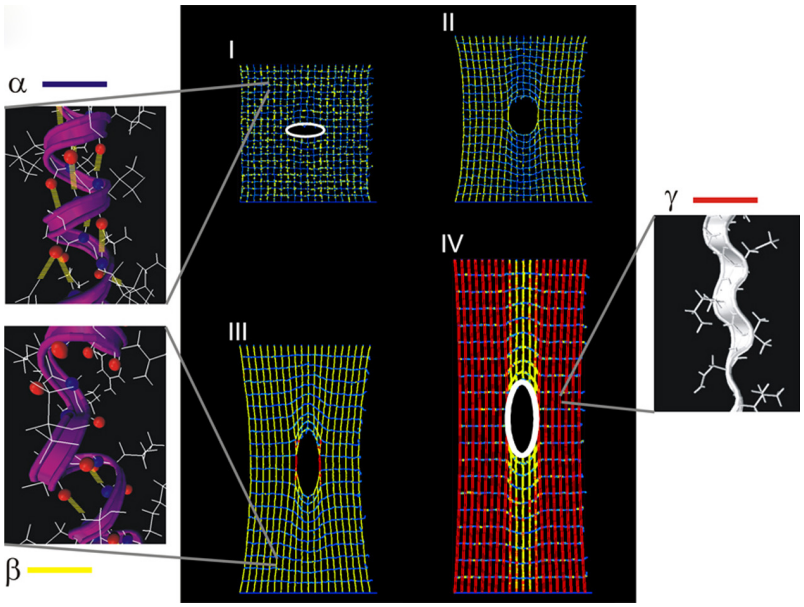

Source: Ackbarow T, Sen D, Thaulow C, Buehler MJ (2009) Alpha-helical protein networks are self-protective and flaw-tolerant. *PLoS One* 4(6): e6015 PMID:19547709.

Figure 6B. Snapshots of the network with crack at different laterally applied strains. The deformation mechanism of the network is characterized by molecular unfolding of the alpha-helical protein domains, leading to the formation of very large plastic yield regions. These plastic yield regions represent an energy dissipation mechanism to resist catastrophic failure of the system. Once the entire structure reaches the rupture strain the crack propagates, leading to catastrophic failure, characterized by breaking of atomic bonds within the peptide backbone of the alpha-helix.

The white ellipsoids in the first (I) and last (IV) images highlight the crack-shape transformation that occurs during deformation (i.e., they show the surface geometry of the crack). Note that the orientation of the ellipsoid shifts from orthogonal to the direction of stretching (image I) to parallel to the direction of stretching (image IV). This has the effect of blunting (rounding out) the crack tip in the vulnerable direction, orthogonal to the direction of the applied strain.

The blowups (labeled α, β, γ) show the nanoscale structural arrangements of the alpha-helical protein filaments under different levels of strain.

The **α structure** is an intact helix, with 3 to 4 hydrogen bonds (H-bonds) per turn (yellowish thick lines). The **β structure** is a partially unfolded alpha-helix, with some of the H-bonds broken along the filament axis whereas others are still intact. The **γ structure** shows a completely unfolded alpha-helix, where the protein's backbone is being stretched. These three structures correspond to the color codes blue (α structure), yellow (β structure), and red (γ structure) in the images (I-IV).

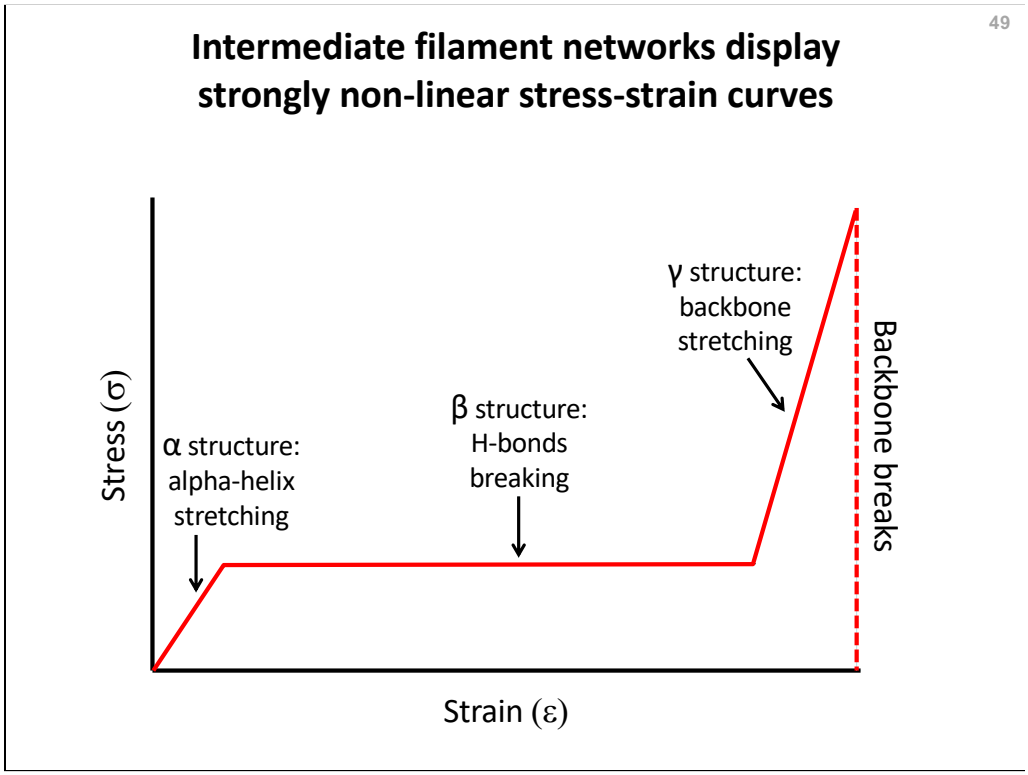

Source: Ackbarow T, Sen D, Thaulow C, Buehler MJ (2009) Alpha-helical protein networks are self-protective and flaw-tolerant. *PLoS One* 4(6): e6015 PMID:19547709.

Figure 6A. Schematic of the characteristic stress-extension curve of a single alpha helix of an intermediate filament protein consisting of three stretching regimes/structures:

(i) **α structure**, stretching of the alpha-heli.

(ii) **β structure**, breakage of H-bonds between adjacent turns of the alpha-helix; successive breakage of each H-bond requires the same amount of energy, which is why the stress-strain curve is flat in this region.

(iii) **γ structure**, stretching of the polypeptide backbone until maximum strain is reached, at which point the alpha-helix backbone breaks.

See slide 49.

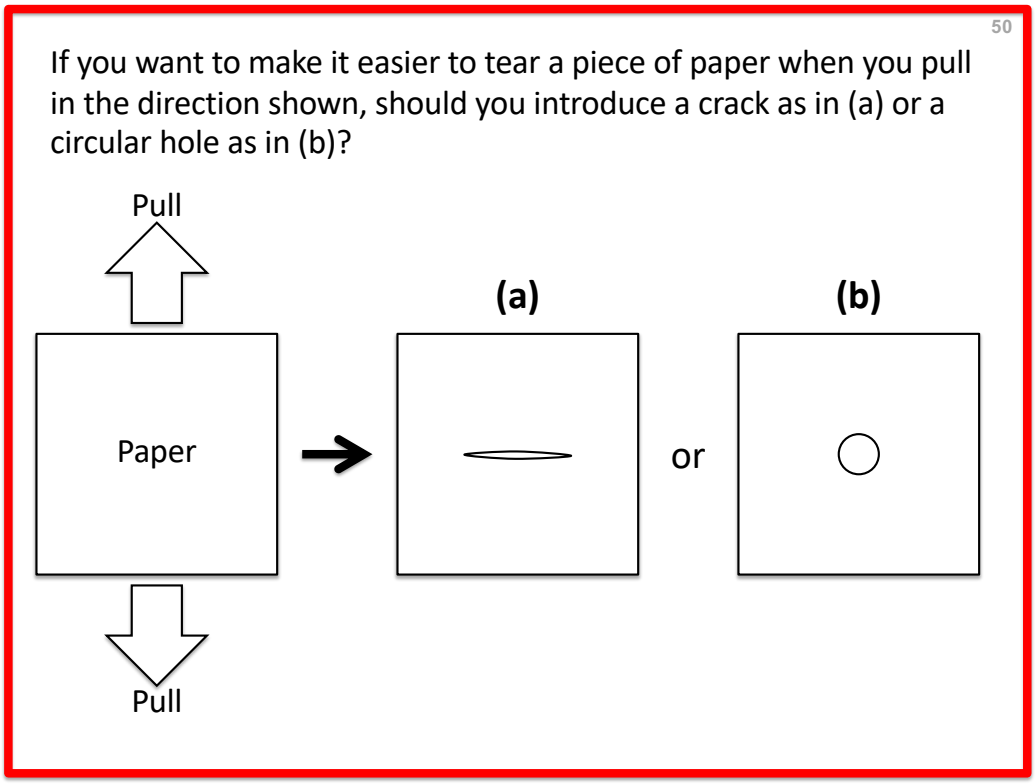

Answer: (a)

Can you explain why?

I encourage you to demonstrate this principle to yourself with a piece of paper and a scissors to make the crack shown in (a) and a hole-punch to make the hole shown in (b). You have just demonstrated how blunting the tip of a crack, as in (b), can protect the material against crack propagation. This is the "secret" underlying the resistance of intermediate filament networks to crack propagation: as shown in slide 45, whichever way you pull on an intermediate filament network, it will stretch to "round out" the leading edge of a crack, thus preventing crack propagation. This is closely related to the "quick fix" practice known in the aircraft industry as "stop drilling": paradoxically, by drilling a hole at the tip of a crack (which introduces more, not less, material damage to the structure!), you can actually prevent the crack from propagating by blunting the crack tip.

For example, see:

Song PS, Shieh YL (2004) Stop-drilling procedure for fatigue life improvement. *International Journal of Fatigue* 26(12): 1333-1339. doi.org/10.1016/j.ijfatigue.2004.04.009

Stopholes suppress crack propagation (because the crack tips are blunted)

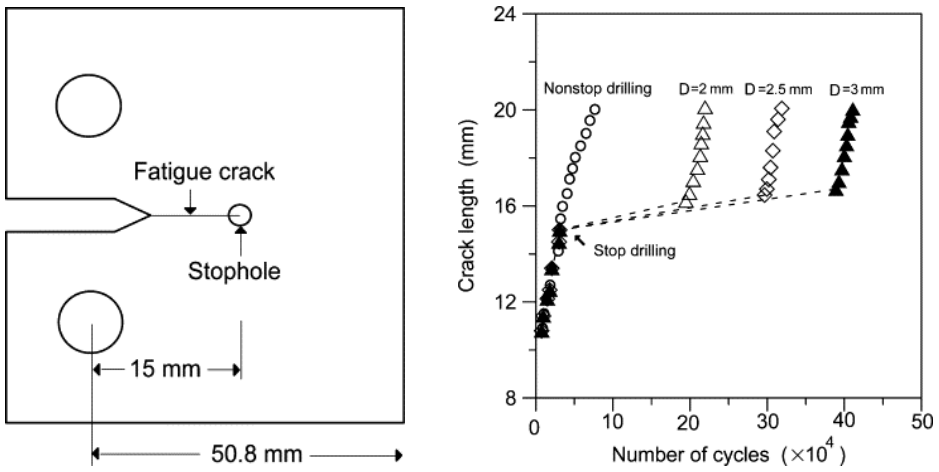

Source: https://www.sciencedirect.com/science/article/pii/S0142112304001045#FIG1